CANCER

Genomic heterogeneity and ploidy identify patients with intrinsic resistance to PD-1 blockade in metastatic melanoma

Giuseppe Tarantino[1,2,3], Cora A. Ricker[1,3], Annette Wang[2], William Ge[2], Tyler J. Aprati[1,3], Amy Y. Huang[1,2,3,4], Shariq Madha[5,6], Jiajia Chen[1,3], Yingxiao Shi[1,2,3], Marc Glettig[1,3], Catherine H. Feng[7], Dennie T. Frederick[3], Samuel Freeman[3], Marta M. Holovatska[1], Michael P. Manos[1], Lisa Zimmer[8], Alexander Rösch[8], Anne Zaremba[8], Elisabeth Livingstone[8], Jacob C. Jameson[9], Soroush Saghafian[10], Andrew Lee[11], Karena Zhao[11], Luc G.T. Morris[11], Brendan Reardon[1,3], Jihye Park[1,3], Haitham A. Elmarakeby[1,3,12], Bastian Schilling[8,13], Anita Giobbie-Hurder[1], Natalie I. Vokes[7], Elizabeth I. Buchbinder[1], Keith T. Flaherty[14], Rizwan Haq[1], Catherine J. Wu[1,2,3,15], Genevieve M. Boland[14], F. Stephen Hodi[1], Eliezer M. Van Allen[1,2,3], Dirk Schadendorf[8]†, David Liu[1,2,3]*†

The introduction of immune checkpoint blockade (ICB) has markedly improved outcomes for advanced melanoma. However, many patients develop resistance through unknown mechanisms. While combination ICB has improved response rate and progression-free survival, it substantially increases toxicity. Biomarkers to distinguish patients who would benefit from combination therapy versus aPD-1 remain elusive. We analyzed whole-exome sequencing of pretreatment tumors from four cohorts (n = 140) of ICB-naïve patients treated with aPD-1. High genomic heterogeneity and low ploidy robustly identified patients intrinsically resistant to aPD-1. To establish clinically actionable predictions, we optimized and validated a predictive model using ploidy and heterogeneity to confidently identify (90% PPV) patients with intrinsic resistance to and worse survival on aPD-1. We further observed that three of seven (43%) patients predicted to be intrinsically resistant to single-agent PD-1 ICB responded to combination ICB, suggesting that these patients may benefit disproportionately from combination ICB. These findings highlight the importance of heterogeneity and ploidy, nominating an approach toward clinical actionability.

INTRODUCTION

The introduction of immune checkpoint blockade (ICB) has markedly enhanced the treatment landscape for patients with advanced melanoma, but only a subset of patients has durable response to therapy (*1*–*3*). Single-agent antibodies to programmed cell-death protein 1 (aPD-1) ICB nivolumab and pembrolizumab and combination aPD-1 and anti-cytotoxic T-lymphocyte associated protein-4 (aCTLA-4) ICB (ipilimumab + nivolumab) are standard first-line treatment options for patients with advanced metastatic melanoma, with the latter showing improved response rates and progression-free survival (PFS) and trending toward improved overall survival (OS) (*4*). However, combination therapy incurs more severe immune-related adverse events (>50% versus ~15% for single-agent aPD-1 ICB) (*3*, *5*), and the absolute difference in proportion of patients with durable response to combination versus single-agent ICB is <10%. Biomarkers to guide between combination and single-agent ICB are crucial but currently lacking. This highlights the need to improve our understanding of the molecular determinants of response and resistance to (i) guide more personalized and rational utilization of ICB treatment options and (ii) identify novel targets and combinations to overcome resistance. Thus far, several markers have been suggested to be associated with response to aPD-1 ICB. Tumor mutational burden (TMB) was the first to be associated with response in patients with melanoma (*6*, *7*). Subsequently, several additional features have been proposed on the basis of neoantigaen load, immunohistochemical quantification of programmed death-ligand 1 (PD-L1) and CD8, genetic alteration in the antigen presentation genes, and gene expression–based interferon-γ (IFN-γ) signature (*7*–*13*). Many of these biomarkers were nominated in nonmelanoma or pancancer settings, with inconsistent validation in metastatic melanoma and without differentiation of important clinical context (e.g., different ICB regimens or prior therapy). In this study, we focus on aCTLA-4 ICB–naïve patients with metastatic melanoma (which represents the current front-line therapy setting for metastatic melanoma) treated with aPD-1 ICB, discovering that genomic heterogeneity and ploidy predict intrinsic resistance to aPD-1 ICB. We develop a simple decision tree based on these features to identify with high precision patients with intrinsic resistance to aPD-1 ICB who may disproportionately benefit from combination ICB and validate these findings in independent

[1]Department of Medical Oncology, Dana-Farber Cancer Institute, Boston MA, USA. [2]Harvard Medical School, Boston, MA, USA. [3]Broad Institute of MIT and Harvard, Cambridge, MA, USA. [4]Computational and Systems Biology Program, Massachusetts Institute of Technology, Cambridge, MA, USA. [5]Worcester Polytechnic Institute, Worcester, MA, USA. [6]Channing Division of Network Medicine, Brigham and Women's Hospital, Boston, MA, USA. [7]Department of Thoracic/Head and Neck Medical Oncology, The University of Texas MD Anderson Cancer Center, Houston, TX, USA. [8]Department of Dermatology, University HospitalEssen, Essen, Germany. [9]Interfaculty Initiative in Health Policy, Harvard University, Cambridge, MA, USA. [10]Harvard Kennedy School, Harvard University, Cambridge, MA, USA. [11]Department of Surgery and Cancer Immunogenomics Research Program, Memorial Sloan Kettering Cancer Center, New York, NY, USA. [12]Al-Azhar University, Cairo, Egypt. [13]Department of Dermatology, University Hospital Würzburg, Würzburg, Germany. [14]Massachusetts General Hospital, Boston, MA, USA. [15]Department of Medicine, Brigham and Women's Hospital, Boston, MA, USA.
*Corresponding author. Email: david_liu@dfci.harvard.edu
†These authors contributed equally to this work.

cohorts of PD-1 and contrast with combination PD-1/CTLA-4 ICB–treated patients with melanoma. We also observe that these predictions do not mirror known clinical or previously nominated molecular features associated with poor-risk disease or poor response to ICB. This work builds on our recent findings, where prior therapy significantly stratified response to aPD-1 ICB, and overcomes prior limitations due to lack of validation cohorts (*14*). The aim is to enhance personalized and rational ICB utilization, identify novel targets and combinations to overcome resistance, and understand the role of genomic heterogeneity and ploidy in response and survival, advancing precision medicine in oncology.

RESULTS

Low ploidy and high heterogeneity discriminate patients with intrinsic resistance to aPD-1 ICB in multiple independent cohorts

We harmonized several cohorts of patients with metastatic melanoma from previous studies and clinical trials (table S1) (*15*, *16*). From these studies, we identified patients matching first-line treatment with aPD-1 immune checkpoint blockade (i.e., removing patients who had prior ICB treatment or were treated with aCTLA-4 or combination aPD-1/aCTLA-4 therapy) with whole-exome sequencing (WES) of pretreatment tumor samples (Materials and Methods). We categorized patients with intrinsic resistance to therapy [exhibiting progressive disease (PD) at first restaging scan] as "progressors." In a previous analysis of WES of patients with metastatic melanoma treated with aPD-1 ICB (*14*), we found that high genomic heterogeneity and low genomic ploidy predicted intrinsic resistance in ICB-naïve patients, and a parsimonious predictive model incorporating genomic heterogeneity, ploidy, and tumor purity predicted intrinsic resistance [cross-validation area under the curve (AUC) of 0.76]. Genomic heterogeneity was defined as the proportion of subclonal nonsynonymous mutations inferred from WES (Materials and Methods).

In the current study, we applied this model to an independent cohort from two clinical trials (BMS CheckMate-038 and CheckMate-064; 27 and 13 patients, respectively, included after quality control), demonstrating a modest AUC of 0.64 (fig. S1A). Examining the individual features of the model, tumor purity was not associated with response in the independent cohorts evaluated (fig. S1B), but the association between higher genomic heterogeneity and lower ploidy with intrinsic resistance to therapy was robust (ploidy MW $P = 0.002$ and heterogeneity MW $P = 0.038$; ploidy MW $P = 0.027$ and heterogeneity MW $P = 0.018$ in the original and independent cohorts, respectively; Fig. 1, A and B). Consequently, we developed models using only the robust features of genomic heterogeneity and ploidy in a combined discovery cohort (Fig. 1C) of $n = 124$ patients. Logistic regression and decision tree models using heterogeneity and ploidy had moderate AUCs in the combined cohort (AUC of 0.73 and 0.75, respectively; 10-fold cross-validation AUC of 0.72; fig. S2); patients predicted to be PD by the model had an overall response rate (ORR) of 5.1 (95% CI, 2.4 to 10.9) and 8.6 (95% CI, 3.7 to 20.1) for intrinsic resistance in the logistic regression and decision tree models, respectively (Fig. 1, D and E). The models also stratified OS and PFS with the patients predicted as PD having worse OS [decision tree hazard rate ratio (HR) = 3.1 (95% CI, 1.8 to 5.3), $P < 0.0001$; logistic regression HR = 1.9 (95% CI, 1.1 to 3.3), $P = 0.019$] and PFS [decision tree HR = 2.5 (95% CI, 1.6 to 3.9), $P < 0.0001$; logistic regression HR = 2.0 (95% CI, 1.3 to 3.1), $P = 0.0018$; fig. S3]. The decision tree model was characterized by higher-precision/positive predictive value (PPV; 76% versus 66%) and specificity (84% versus 71%) compared to the logistic regression model (fig. S2, B and C), offering a straightforward approach to predicting patients with intrinsic resistance (Fig. 1F).

To further evaluate the robustness and potential translatability of our findings, which were based on our methods to infer genomic heterogeneity and ploidy from WES, we evaluated multiple different definitions of genomic heterogeneity, specifically varying the cancer cell fraction (CCF) thresholds to categorize variants "clonal" versus "subclonal" and different metrics of heterogeneity, and found that our results remained robust across a range of thresholds and heterogeneity metrics (Materials and Methods, fig. S4, and table S2). Furthermore, we tested an automated approach to infer purity and ploidy (needed to estimate CCF), with significant stratification between progressors and responders (Materials and Methods and fig. S5), suggesting potential feasibility for practical applications.

Timing of whole-genome doubling event distinguishes responders versus nonresponders with whole-genome doubling

We analyzed tumors misclassified by our model, e.g., tumors exhibiting low heterogeneity and high ploidy but still showing intrinsic resistance, and tumors with high heterogeneity and low ploidy but without intrinsic resistance. The distribution of ploidy in our cohorts is bimodal (Fig. 2A and fig. S6), with higher ploidy driven by whole-genome doubling (WGD) events (Fig. 2, A and B). The mutations within WGD tumors manifest different multiplicities (e.g., one or two copies per cancer cell) reflecting mutations occurring either after (one copy) or before (two copies) the WGD event (Fig. 2C). Consequently, the ratio of 2:1 multiplicity of mutations is thus associated with time from the WGD event (*17*, *18*). Three WGD tumors, misclassified by our predictive model as nonprogressors because of low heterogeneity and high ploidy, exhibited a high 2:1 single-nucleotide variant (SNV) multiplicity ratio. This suggests that they may represent recent WGD events (Fig. 2D). Incorporating SNV multiplicity as a feature of the model led to a small AUC improvement (AUC = 0.76; fig. S7, A and B, with examples of PD samples with WGD and low heterogeneity in fig. S7C and responder samples with WGD and low heterogeneity in fig. S7D). Conversely, misclassified patients predicted to have intrinsic resistance (PD) but observed to have non-PD (nPD; 11 of 46 predicted PD patients) lacked distinguishable genomic or clinical characteristics. Most of these patients had stable disease (SD) as best response [7 SD, 3 partial response (PR), and 1 complete response (CR) of 11 misclassified patients]. Furthermore, most misclassifications occurred at relatively lower heterogeneity (fig. S8), indicating less favorable outcomes, even in the absence of PD at the earliest assessment point.

Genomic heterogeneity specifically predicts therapy response, while ploidy is prognostic

To probe the distinct prognostic (i.e., indicative of poor biology independent of therapy) and predictive (outcome in the context of therapy) functions of genomic heterogeneity and ploidy, we examined data from The Cancer Genome Atlas (TCGA) melanoma cohort (*19*). This information was gathered at a time when modern targeted and ICB therapies were not broadly used, thus representing an "untreated" cohort. Ploidy was significantly higher in metastatic

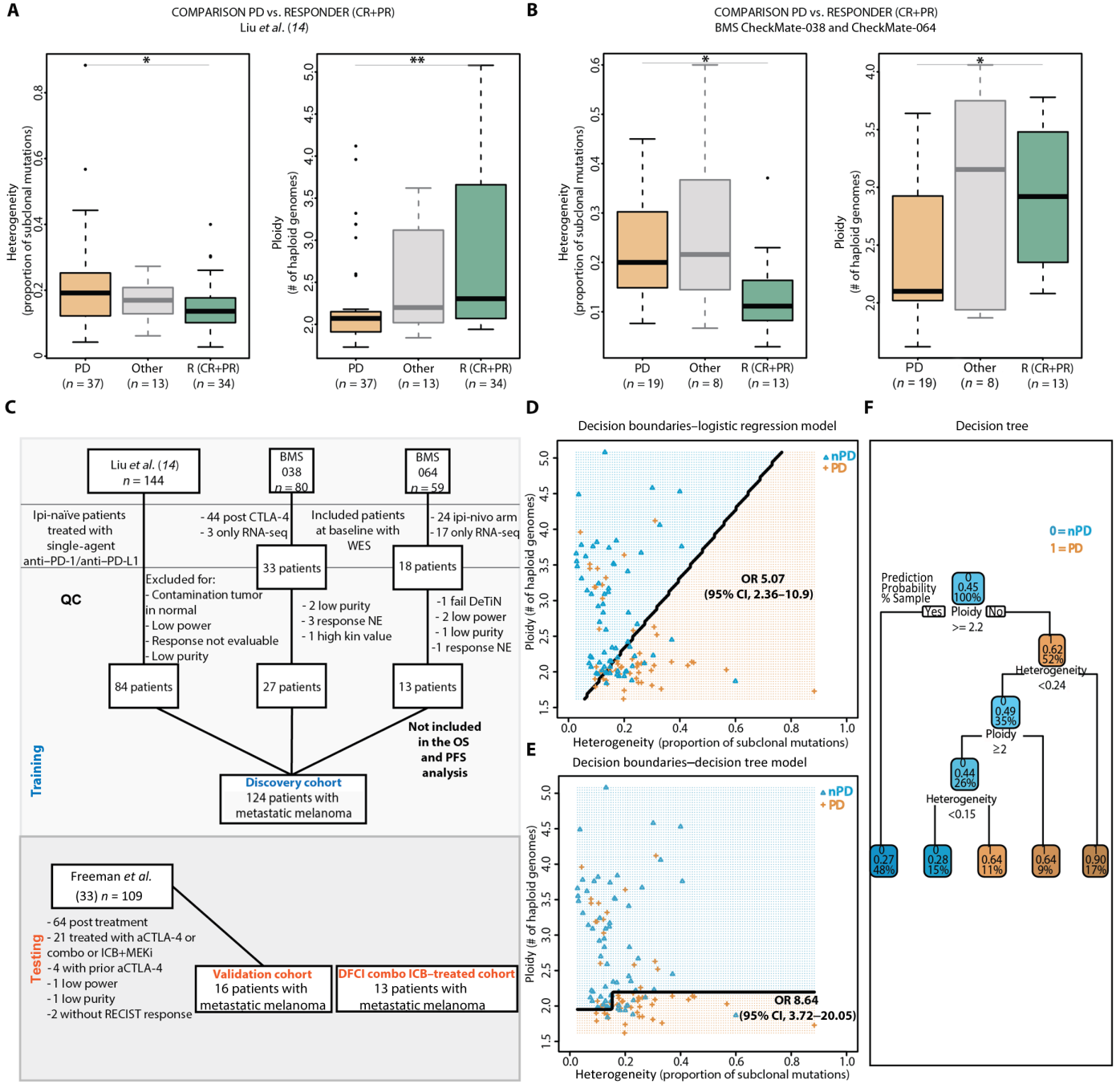

Fig. 1. High genomic heterogeneity and low ploidy predict intrinsic resistance in previously ICB-naïve PD-1 treated patients. (**A**) Genomic heterogeneity and ploidy in progressors (PD as best response, orange) versus responders (CR/PR as best response, green) and other (SD or MR as best response, gray) in the CTLA-4 ICB–naïve PD-1 ICB–treated subset of a large discovery cohort of patients with metastatic melanoma [Mann-Whitney Wilcoxon (MWW) $P = 0.038$ and $P = 0.0021$ for heterogeneity and ploidy, respectively]. (**B**) Genomic heterogeneity and ploidy comparison in progressors, other, responders of a validation CTLA-4 ICB–naïve PD-1 ICB–treated cohort drawn from two clinical trials (MWW $P = 0.018$ and $P = 0.027$ for heterogeneity and ploidy, respectively). (**C**) A combined discovery cohort was constructed combining the patients from three different cohorts: (*14*), the clinical trials CheckMate-038 and CheckMate-064. For CheckMate-064, only the patients in the arm A were selected; for these patients, the response was evaluated after 12 weeks. (**D**) Decision boundaries of the logistic regression model (LR) with genomic heterogeneity and ploidy as features to predict patients with intrinsic resistance (PD) using the combined discovery cohort. The orange area represents the area predicted by the model as PD, while the blue area represents the patients predicted as not PD (nPD). The observed therapy response of each patient is represented by the orange plus symbol (PD) or the blue triangle (nPD). (**E**) Decision boundaries for a decision tree model. (**F**) Structure of the decision tree with logic and split cutoff used. In each node, the top number represents the overall prediction for the node, with 1 being PD and 0 being nPD. The second number represents the probability of the patients in that group to be PD. The third number denotes the proportion of samples in that node.

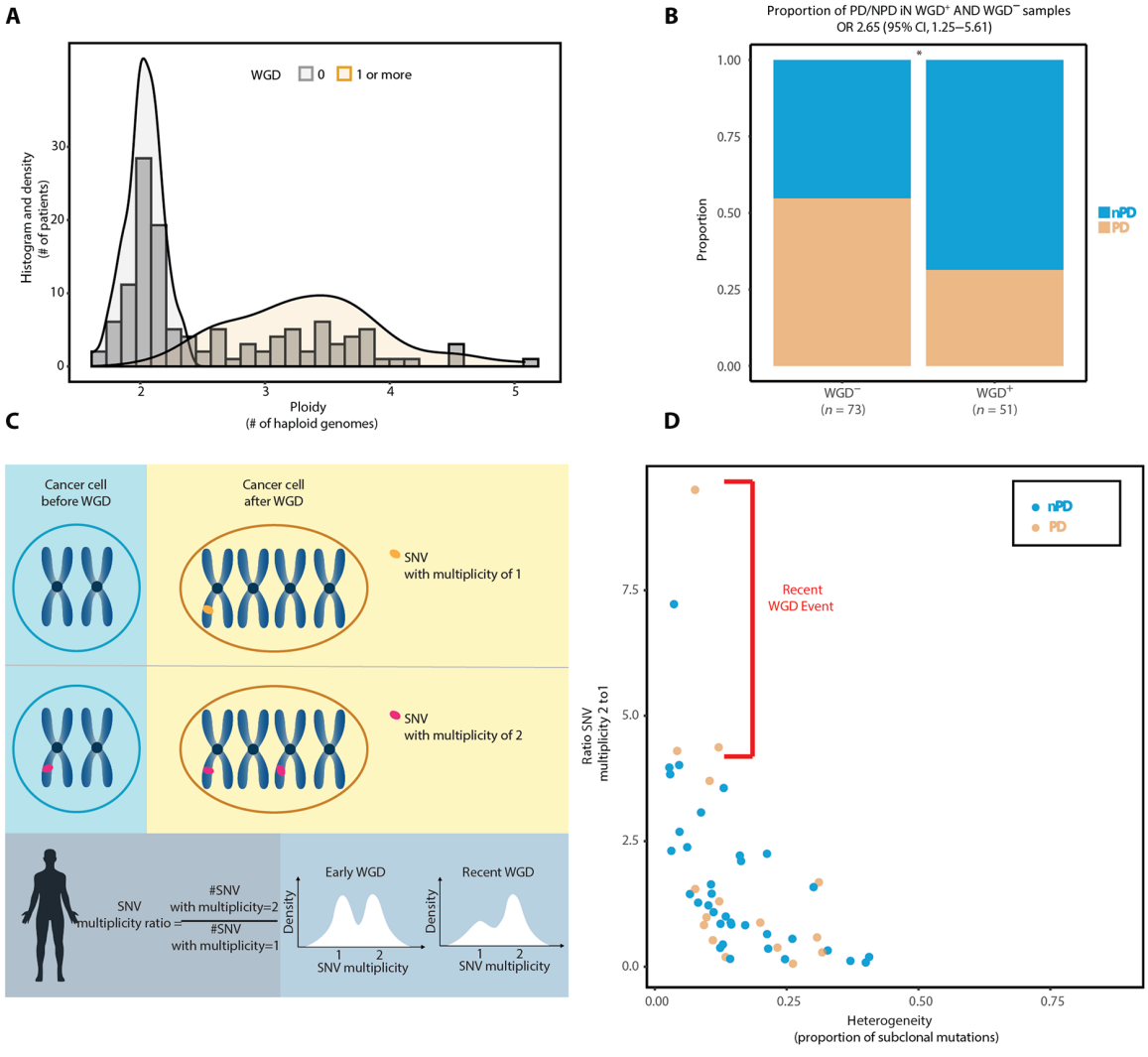

Fig. 2. WGD and its timing are associated with response to ICB. (**A**) Ploidy distribution of whole-genome doubled and non–whole-genome-doubled tumors. Higher ploidy is driven by WGD events. (**B**) Proportion of patients with WGD event in the patients with PD versus nPD patients (Fisher's exact $P = 0.011$). (**C**) Graphical representation on how to compute the SNV multiplicity ratio and estimate the time of WGD event. (**D**) Ratio of multiplicity 2:1 SNV mutations and heterogeneity scatterplot for WGD tumors. Orange dots represent patients with PD as best response (PD), and blue represents nPD. A high 2:1 SNV multiplicity ratio indicates few SNV mutations after genome doubling, consistent with a recent WGD event.

($n = 392$) versus primary ($n = 61$) lesions (Fig. 3A), a finding in line with previous studies (*14*, *20*, *21*), which underscores the role of WGD in tumor development and metastasis (*22*). In contrast, genomic heterogeneity was significantly higher in primary samples (Fig. 3A), consistent with a founder bottlenecking effect in metastatic lesions. Univariate Cox survival analyses of the metastatic subset revealed that ploidy, but not heterogeneity, was associated with OS [heterogeneity HR = 1.5 (95% CI, 0.55 to 4.0), $P = 0.44$, ploidy HR = 0.76 (95% CI, 0.6 to 0.96), $P = 0.02$; Fig. 3, C and D]. In contrast, in our aPD-1 ICB–treated cohort, high heterogeneity in metastatic samples was strongly associated with worse PFS and OS [PFS Cox HR = 8.0 (95% CI, 1.5 to 42), $P = 0.013$; OS Cox HR = 19.0 (95% CI, 4.1 to 84)]. Ploidy displayed a similar estimated effect size and borderline statistically significant associations with improved PFS [Cox HR = 0.74 (95% CI, 0.54 to 1), $P = 0.065$] and OS [Cox HR = 0.76 (95% CI, 0.51 to 1.1), $P = 0.181$] in this smaller cohort. In multivariate analysis, ploidy (but not heterogeneity) once again predicted OS in the untreated cohort [HR = 0.64 (95% CI, 0.5 to 0.84), $P = 0.001$; Fig. 3E], whereas in the aPD-1 ICB–treated cohort, heterogeneity strongly stratified PFS and OS, while ploidy lost its predictive strength [heterogeneity HR = 13.87 (95% CI, 2.7 to 71.3), $P = 0.002$; ploidy HR = 0.87 (95% CI, 0.56 to 1.4), $P = 0.55$; Fig. 3, F and G]. Collectively, our analysis demonstrates the strong predictive role of genomic heterogeneity on patient outcomes under aPD-1 ICB therapy, while ploidy is also prognostic in non-ICB–treated scenarios.

Genomic heterogeneity is higher in noncutaneous melanoma subtypes and is driven by non-ultraviolet mutational processes

In our investigation, we examined the differences in genomic heterogeneity and ploidy among the different types of metastatic melanoma, including the following subtypes: cutaneous ($n = 90$), acral

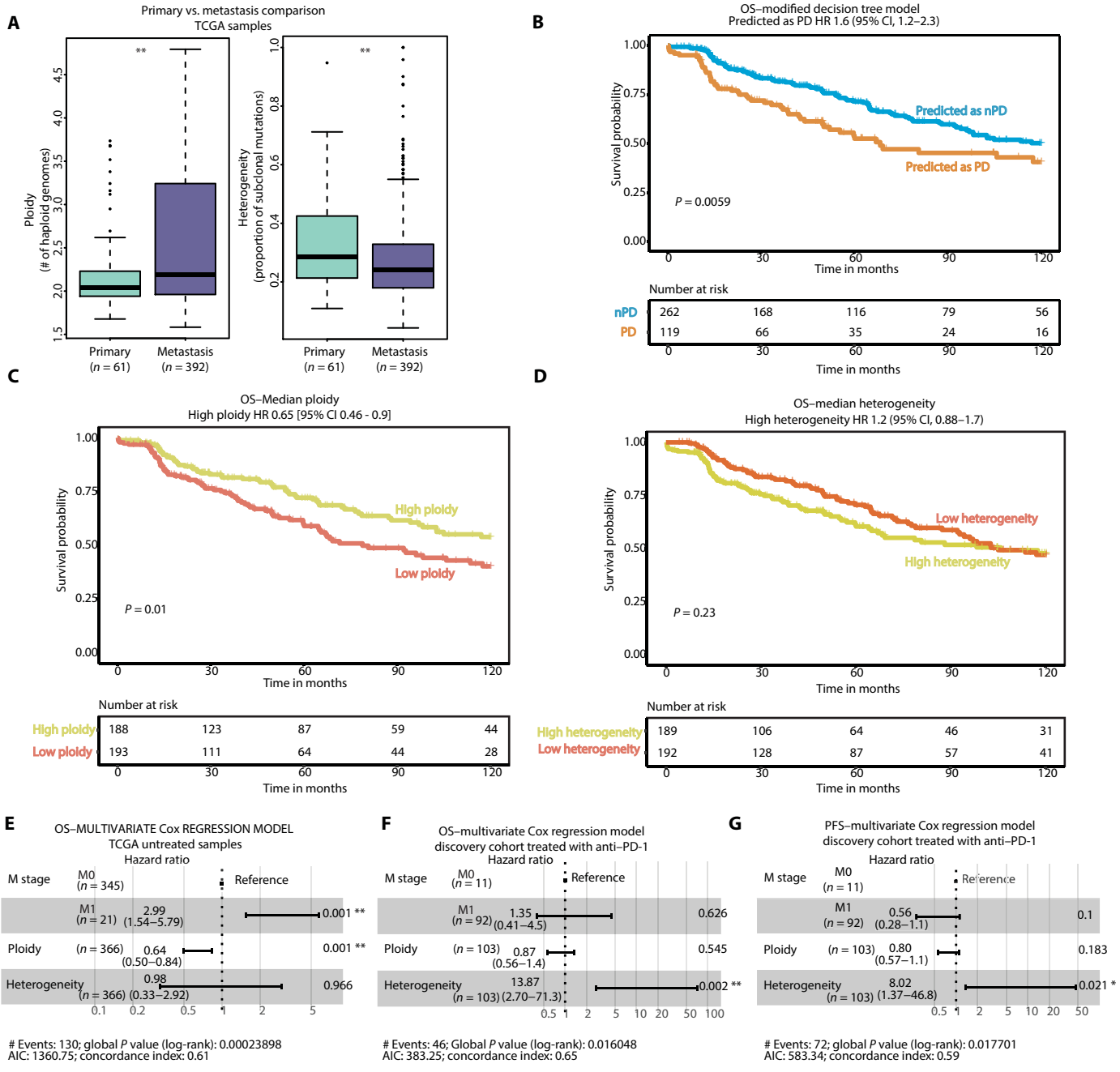

Fig. 3. Association of heterogeneity and ploidy with survival in ICB-treated and ICB-untreated cohorts. (**A**) Difference in genomic heterogeneity and ploidy between primary and metastatic ICB-untreated samples in TCGA melanoma cohort (MWW $P = 0.0031$ and $P = 0.0062$ for heterogeneity and ploidy, respectively). (**B**) OS survival of the TCGA samples stratified by predicted PD status using the modified decision tree model. (log-rank $P = 0.0059$). (**C**) OS survival of the TCGA samples stratified by median ploidy (log-rank $P = 0.01$). (**D**) OS survival of the TCGA samples stratified by median heterogeneity (log-rank $P = 0.23$). (**E**) Multivariate Cox regression model evaluating the effect of ploidy and heterogeneity for the OS in the TCGA cohort. (**F**) Multivariate Cox regression model evaluating the effect of ploidy and heterogeneity for the OS in the anti–PD-1 discovery cohort. (**G**) Multivariate Cox regression model evaluating the effect of ploidy and heterogeneity for the PFS in the anti–PD-1 discovery cohort.

($n = 9$), occult and other ($n = 14$), mucosal ($n = 9$), and ocular/uveal ($n = 2$). Our analysis revealed that acral melanoma exhibits the highest incidence of WGD, at 55%, followed by mucosal at 44% and cutaneous at 40%. These trends are consistent with recent whole-genome sequencing studies (*23*). Notably, our data indicate that noncutaneous melanoma subtypes show significantly higher heterogeneity compared to cutaneous melanomas. Specifically, the median heterogeneity is 0.27 for acral melanoma ($P = 0.021$), 0.43 for patients with ocular/uveal melanoma ($P = 0.025$), although this is based on a small sample size, and 0.3 for the mucosal group ($P < 0.001$), in contrast to a median heterogeneity of 0.15 in cutaneous melanoma (fig. S9). However, associations between heterogeneity and ploidy with response were evident even when confining the analysis to cutaneous melanoma (heterogeneity $P = 0.013$; ploidy

$P < 0.001$; fig. S9D). Mutational signature analysis demonstrated a positive correlation of genomic heterogeneity with a double-strand break–related mutational signature (COSMIC Signature 3) (*24*), and negative correlation with the proportion of mutations inferred to be due to the ultraviolet (UV) mutational signature (COSMIC Signature 7; fig. S10) (*24*), suggesting that genomic heterogeneity in cutaneous melanomas is driven by non–UV-associated mutational processes after the appearance of the initial melanoma clone driven primarily by UV-induced mutations.

Heterogeneity and ploidy can better identify patients with PD compared to previously nominated signatures and biomarkers

TMB and an IFN-γ signature have been associated with response to aPD-1 ICB in large pancancer cohorts (*10*), although performance in the melanoma subgroup was worse than the pancancer cohort (AUC of 0.60, 0.64, and 0.66 for TMB, IFN-γ signature, and the combination, respectively). In our cohort of patients with metastatic melanoma, we explored the stratification of responders (CR+PR) versus PD in terms of TMB and IFN-γ. In the studies of the individual cohorts in our combined discovery cohort, the association of TMB with response to therapy was mixed (*14*, *25*). A predictive model using TMB and IFN-γ signature in the subset of our discovery cohort with bulk RNA sequencing (RNA-seq; $n = 108$; fig. S11) had moderate performance (AUC = 0.67) but was worse both in terms of AUC and Bayesian Information Criteria (BIC) in comparison with a model with genomic heterogeneity and ploidy (figs. S12 and S13). Notably, one of the highest TMB tumors (>50 mutations per MB) was a nonresponder but had high heterogeneity and low ploidy (fig. S12) and was correctly classified by our model. While TMB, estimated as total number of nonsynonymous mutations, is independent of heterogeneity and ploidy (fig. S14), its inclusion in the model with heterogeneity and ploidy did not substantially enhance performance (AUC increase of 0.0063). Among a subgroup of patients for whom the RNA-seq data were available, TMB and IFN-γ were not correlated with ploidy and heterogeneity, IFN-γ does not improve model performance, while TMB led to a marginal AUC improvement in the subset with RNA-seq data (AUC increase of 0.0163; figs. S12, S13, S15 and S16).

Unbiased feature selection reveals a signature of tertiary lymphoid structures as a potential additional model feature

To further examine other more recently nominated features, we evaluated recently described transcriptomic signatures and models, different metrics of genomic instability, and a thorough examination of the correlations between all the features evaluated (full list in table S3; figs. S12 to S14). We also tested recent tumor states signatures (fig. S17A) (*26*, *27*). The analysis led to the identification of a significant association between the melanocytic state signature and PD to single-agent aPD-1 ($P = 0.031$) in both bulk RNA-seq and the tumor-specific transcriptome after deconvolution (Materials and Methods and fig. S17C). A multivariate model including ploidy and heterogeneity together with the melanocytic state showed that these three features are independent from each other (fig. S17B). The melanocytic state does not correlate with ploidy, heterogeneity, or tumor purity or with various immune signatures (fig. S14), suggesting that this association is distinct from tumor immunogenicity.

To evaluate the robustness of these features, we conducted an unbiased forward selection procedure using 10-fold cross-validation, selecting in each fold the model with the lowest BIC and evaluating the frequency of the features across the folds. This evaluation was performed for both subsets with paired WES and RNA-seq ($n = 108$ with 10-fold cross-validation) and the entire discovery cohort ($n = 124$). Specifically, we assessed the best-performing models and their features using 10-fold cross-validation with forward feature selection based on BIC. While ploidy, heterogeneity, and TMB were, as expected, frequently selected features (selected in 10 of 10, 6 of 10, and 7 of 10 of the folds, respectively; the melanocytic state signature was selected only in 2 of 10; fig. S13C), a recent signature of tertiary lymphoid structures (TLSs) (*28*) was selected in 9 of 10 folds. The TLS signature was not associated with intrinsic resistance in univariate analyses. Furthermore, it had relatively low correlation with other immune signatures (fig. S15), suggesting a distinct immunological state. Overall, our analyses suggest additional features that may comprise part of a combination biomarker along with heterogeneity and ploidy.

Optimizing the predictive model identifies patients with intrinsic resistance with high specificity

A barrier to using biomarker-driven strategies clinically is biomarker specificity. We developed a model to predict patients with intrinsic resistance to aPD-1 ICB with high specificity (i.e., strong precision or PPV) at a cost of reduced sensitivity (i.e., accurately pinpointing all patients with intrinsic resistance). This approach reflects a clinical interest in discerning patients highly likely to exhibit intrinsic resistance to single-agent aPD-1 ICB, who might be particularly suited for combination immunotherapies. In alignment with this objective, we developed a modified version of the decision tree model (MDT; Materials and Methods) with increased weights for patients without intrinsic resistance to aPD-1 ICB (Fig. 4A and fig. S8B). Applying this model, 21 patients (comprising 17% of the cohort) were predicted to be PD, with a PPV of 90% (19 of 21 correctly predicted), a specificity of 97% (66 of 68 patients correctly identified as nPD), and a sensitivity of 33% (19 of 56 patients with PD). A modified cross-validation by training on two cohorts and using the third as a validation showed median PPV, specificity, and sensitivity of 0.75, 0.85, and 0.5 (fig. S18). The models stratified OS and PFS, with those predicted as PD having notably worse OS [MDT HR = 3.0 (95% CI, 1.6 to 5.5), $P = 0.00023$] and PFS [decision tree HR = 3.0 (95% CI, 1.7 to 5.2), $P < 0.0001$; Fig. 4B, fig. S8C].

Patients predicted as intrinsically resistant to aPD-1 ICB have similar clinical features to the overall cohort

Certain clinical characteristics such as high tumor burden, site-specific metastases (e.g., brain and liver) indicative of more severe disease, and subtypes such as uveal melanoma are linked with unfavorable outcomes and have clinical indications for combination ICB treatment (*29*–*31*). To assess whether our model's predictions of intrinsic resistance to aPD-1 ICB are independently informative with these adverse clinical features, we examined factors including M stage, lactate dehydrogenase (LDH) baseline levels, the presence of brain metastases, primary melanoma subtype, the presence of liver metastases, Eastern Cooperative Oncology Group (ECOG) performance status, the presence of lung metastases, and age (fig. S19). Notably, our analysis did not uncover any statistically significant differences in clinical characteristics between patients predicted to be PD and others within the cohort (Fig. 4C). In addition, of the 21 patients predicted as PD only, 8 had known clinical features (2 with brain metastases, 2 with uveal melanoma, and 4 with

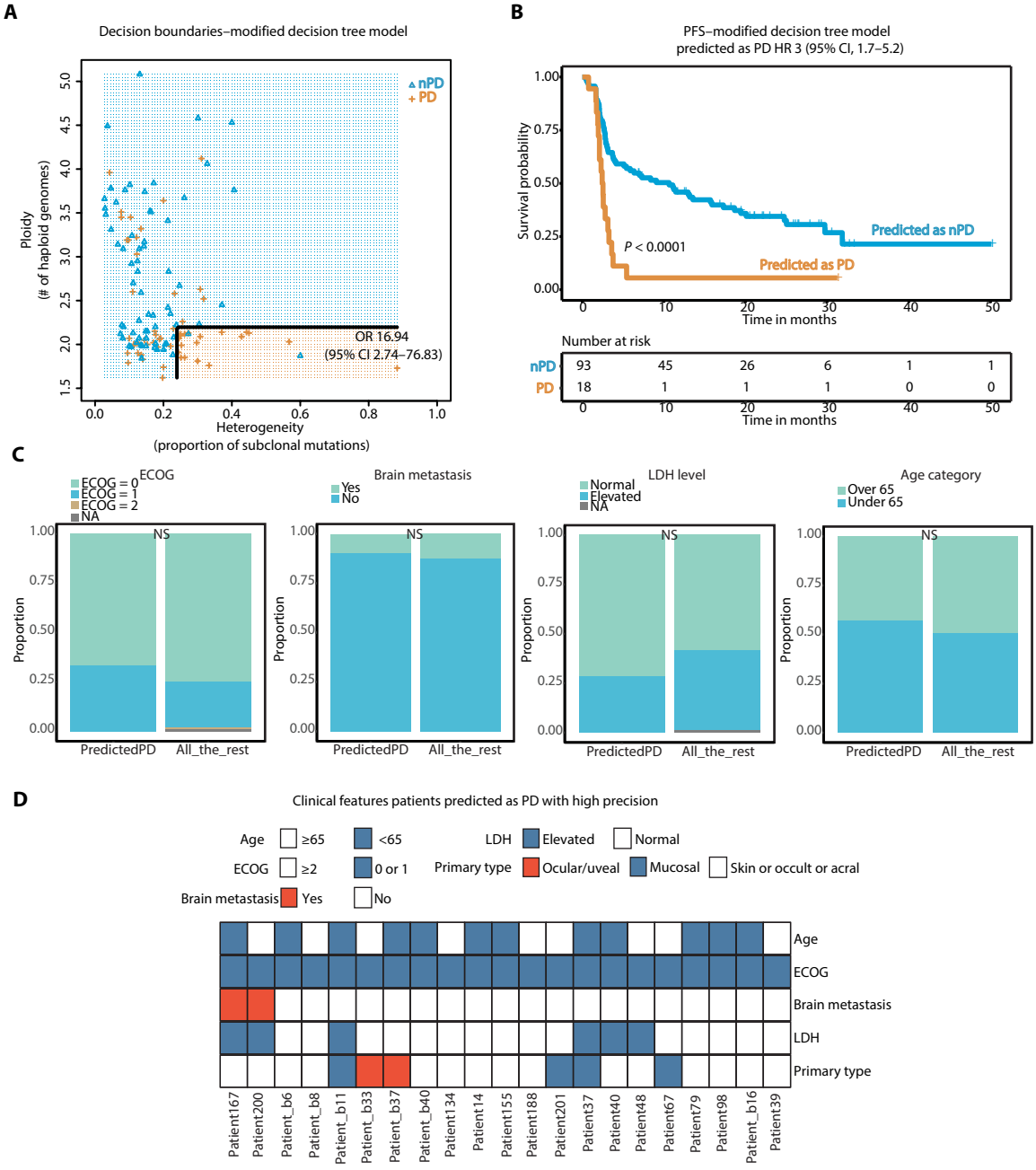

Fig. 4. Constructing a modified decision tree model optimizing precision and specificity for predicting intrinsic resistance to PD-1 ICB. (**A**) Decision boundaries of the MDT model. (**B**) PFS curve stratified by patients predicted by the MDT model as PD (orange) and nPD (blue) (log-rank $P < 0.0001$). In the survival analysis, the samples from CheckMate-064 that received sequential treatments have been excluded ($n = 13$). (**C**) Clinical characteristics between predicted patients with PD ($n = 21$) and the rest of the cohort, comparing ECOG, the presence of brain metastasis, lactate dehydrogenase (LDH) level at baseline and age category. *P* values are from Fisher's exact test. (**D**) Clinical features of the 21 patients predicted as PD. Only four patients (highlighted in red) have clinical features (brain metastasis, ocular/uveal primary type) that strongly indicate combination ICB.

mucosal melanoma) that would strongly argue for the selection of combination ICB (Fig. 4D and table S1). We did not detect significant variations in heterogeneity and ploidy in relation to M stage, LDH level, or between patients with and without brain metastases (figs. S20 and S21). In sum, our model predicts patients to have intrinsic resistance independently of clinical features that might already drive use of combination aPD-1 ICB.

Genomic heterogeneity and ploidy add independent information to a clinical nomogram

Last, we evaluated a recently developed clinical nomogram (*32*) that predicts response to ICB based on clinical features. Unfortunately, our cohort did not have all the required clinical features for the model (i.e., neutrophil-to-lymphocyte ratio, liver metastasis presence, ECOG, and lung metastasis presence). However, five patients

that were correctly predicted by our model to have intrinsic resistance had at least a score of intermediate or good response risk by the nomogram based on available clinical data (fig. S22), emphasizing the additional predictive value of this genomic data.

Independent cohorts validated the model

Last, to validate this model in an external cohort, we collected and tested our model against a small independent cohort of 16 additional patients who were ipilimumab naïve and treated with aPD-1/aPD-L1 (table S4) (*33*). Within this group, we observed 4 patients with CR/PR, 1 patient with SD, 1 patient with a mixed response (MR), and 10 patients with PD as best objective response (BOR). Despite the small sample size, the combination of high heterogeneity and low ploidy effectively pinpointed intrinsically resistant patients (Fig. 5, A to C). Furthermore, our modified model maintained its precision, accurately predicting all patients identified by our optimized approach as intrinsically resistant ($n = 5$, PPV = 100% and specificity = 100%). We further applied our model to an independent cohort of combination aPD-1/aCTLA-4 ICB–treated patients ($n = 13$; table S5). Because of the unavailability of RECIST annotation for this group, we classified intrinsic resistance (PD) as patients who showed progression with a PFS of less than 6 months, contrasting them with those with a PFS exceeding 6 months (nPD). In this cohort of combination aPD-1/aCTLA-4–treated patients, heterogeneity still exhibited a trend toward being elevated in PD patients versus nPD ($P = 0.052$; Fig. 5D), ploidy showed no substantial difference. Three of seven (43%) patients predicted to be intrinsically resistant to single-agent PD-1 ICB by our model turned out to be nPD when treated with the combination aPD-1/aCTLA-4 ICB. This observation suggests that some patients identified by this model might derive differential benefits from combination ICB as opposed to single-agent ICB (Fig. 5E).

Genomic heterogeneity and ploidy can be estimated from clinical assays

Intratumoral heterogeneity and ploidy are estimated here using WES of matched tumor and normal tissue and associated analytics, which are not standardized or routinely available clinically. Targeted next-generation sequencing (TNGS) panels are NGS assays that sequence only a subset of common cancer genes and are used clinically to determine eligibility and efficacy for targeted therapies. The number of genes and genomic area covered by TNGS panels varies widely, from a few dozen genes to several hundred, with a coverage of at most 1 to 3 Mb, in comparison to WES where ~20,000 genes and ~30 Mb are covered, and it is unclear whether genomic heterogeneity and ploidy can be accurately estimated from this reduced coverage or whether such estimates will be predictive of ICB response. To test the potential of TNGS to estimate heterogeneity, we created pseudo-targeted panels by down-sampling WES analysis, taking only the genes included in three TNGS panels: OncoPanel (447 genes), a targeted NGS used at one institution, Foundation Medicine (324 genes), and Essen University Hospital target panel (611 genes). Our analysis showed a very strong correlation between heterogeneity estimates from WES and the pseudo-targeted gene panel, especially when filtering out the samples with less than three mutations detected from TNGS (corr ≥ 0.71, $P < 0.001$ for all the panels; fig. S23). However, a subset of tumors ($n = 44$) were observed with TNGS heterogeneity of 0 but high WES heterogeneity (from 0.02 to 0.4). Tumors with TNGS heterogeneity of 0 had lower TMB (fig. S23D), suggesting that subclonal mutations in genes not included in TNGS panels are nonetheless informative.

To further evaluate the potential estimation of ploidy and heterogeneity from TNGS, we determined naïve estimates of genomic heterogeneity and ploidy using a recently published cohort of ICB-treated patients with MSK-IMPACT targeted panel sequencing, including 22 patients with metastatic melanoma that were ipilimumab naïve and treated with aPD-1. The MSK-IMPACT TNGS uses both the tumor and the matched normal sample, enabling improved copy number estimation. Tumor purity and ploidy were estimated using FACETS (Materials and Methods), and CCF for variants was inferred and used to define subclonal and clonal mutations and, therefore, genomic heterogeneity. Even in this case, 9 of 22 samples had heterogeneity equal to zero, with a clear difference in the heterogeneity distribution compared to our WES discovery cohort (fig. S24A). The distribution of ploidy instead was concordant with that of our discovery cohort, and there is a trend of higher ploidy in nPD samples ($P = 0.21$; fig. S24B), supporting the utilization of paired tumor-normal TNGS to estimate ploidy.

DISCUSSION

In this study, we identified and validated low ploidy and high genomic heterogeneity as two robust independent biomarkers of intrinsic resistance to aPD-1 as first-line ICB in patients with metastatic melanoma across multiple independent cohorts. Comparing with an untreated metastatic melanoma cohort, we found that genomic heterogeneity is predictive of survival in aPD-1–treated populations, while ploidy is prognostic, associated with OS differences even in untreated patients. In addition, we observed that rare melanoma subtypes [which have worse outcomes to immunotherapy (*34*)] have higher genomic heterogeneity, suggesting that this may underpin some of the differences in outcomes. Benchmarking against nominated biomarkers such as TMB and IFN-γ, we find that genomic heterogeneity and ploidy perform better in predicting response and intrinsic resistance. Toward clinical translation, we developed an optimized model with genomic heterogeneity and ploidy to identify with high specificity and PPV patients with intrinsic resistance to single-agent aPD-1 ICB. The majority of patients thus identified had no other adverse clinical feature that would have already predisposed toward combination ICB, and a recent clinical nomogram would have identified these patients as good or intermediate response risks. Furthermore, the timing of the WGD event, as the principal driver of ploidy disparities, may influence predictions of response and survival to aPD-1 ICB.

Intratumoral genomic heterogeneity has been associated with highly mutagenic disease with a higher likelihood of preexisting or rapidly evolving resistant clones and associated with worse clinical outcomes in a range of clinical contexts (*14*, *35*–*38*). In vivo studies of intratumoral heterogeneity using mixes of UVB-irradiated subclones have demonstrated increased tumor growth in heterogeneous compared to homogenous tumors in immune-competent versus immunodeficient mice (*39*). However, it has variable association with response to ICB in different histologies and clinical contexts, and its utility as a biomarker has not previously been well demonstrated. The role of ploidy is much more complex. Large-scale differences in ploidy are driven by WGD events, which are common in cancer [30% of solid tumors in one estimate (*20*)]. The hypothesized benefit of WGD to tumors is the ability to tolerate copy number alterations (aneuploidy) across the genome to find more favorable genomic states (*22*) and mitigate the accumulation

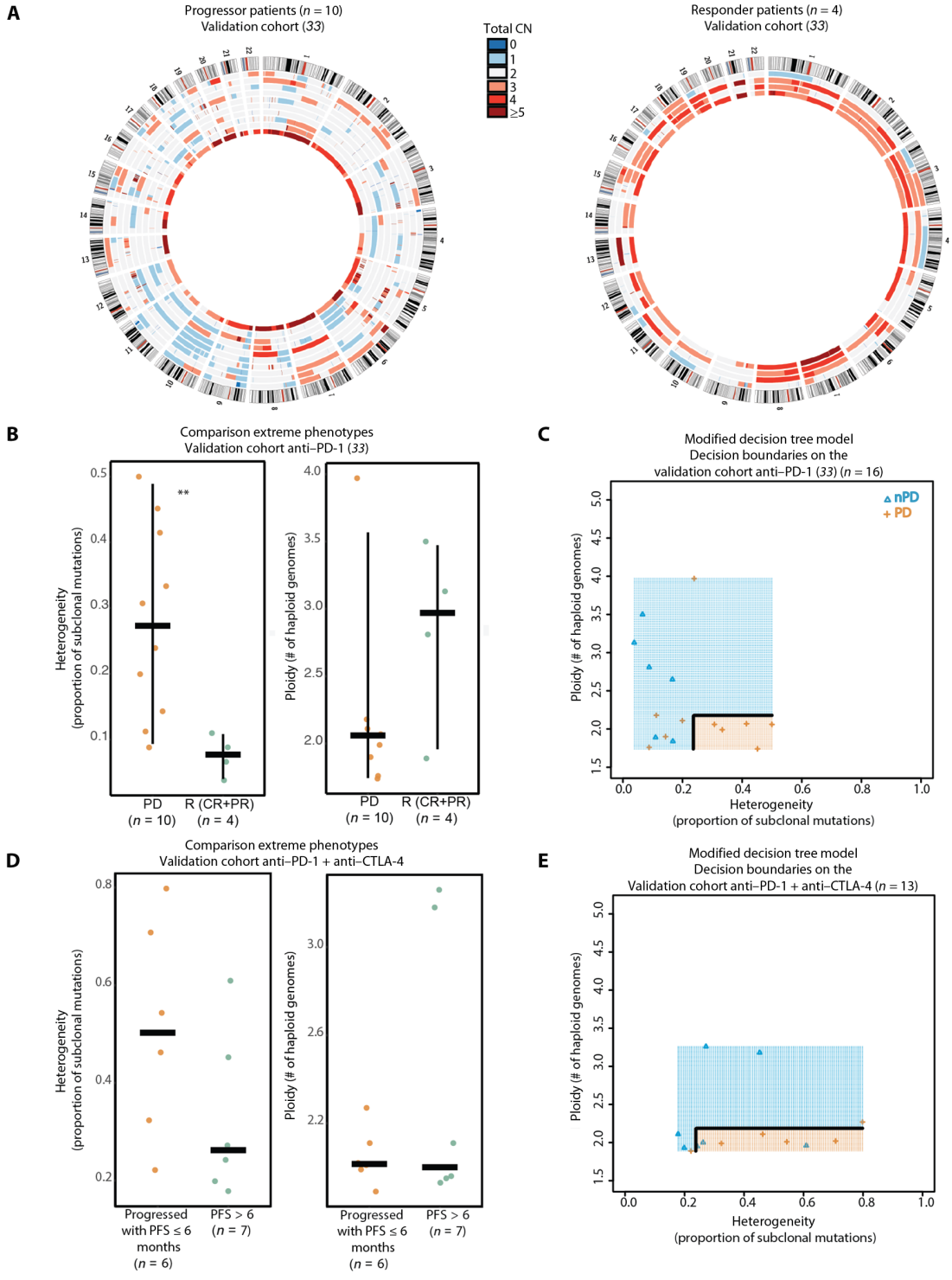

Fig. 5. Association of heterogeneity, ploidy, and predicted PD-1 ICB intrinsic resistance with ICB response in independent validation cohorts. (**A**) Circos plots of copy number alterations in progressors (PD as best response, left) and responders (CR/PR as best response, right) in a PD-1 ICB–treated validation cohort (*33*). (**B**) Heterogeneity and ploidy compared in progressors versus responders in the validation PD-1 ICB cohort (MWW $P = 0.008$ and $P = 0.23$ for heterogeneity and ploidy, respectively) (*33*). (**C**) Decision boundaries for the modified decision tree model using the samples from the validation anti–PD-1 ICB cohort (*33*). (**D**) Heterogeneity and ploidy compared in responders (PFS > 6 months) versus progressors (PFS ≤ 6 months) in a combination PD-1/CTLA-4 ICB cohort (MWW $P = 0.1$ and $P = 1$ for heterogeneity and ploidy, respectively). (**E**) Decision boundaries for the modified decision tree model using the samples from the combination PD-1/CTLA-4 ICB cohort showing response in three of seven patients predicted to be intrinsically resistant to PD-1 ICB.

of deleterious somatic alterations (*40*). In this study, we observe WGD and increased aneuploidy at later tumor stages (Fig. 4A) and longitudinally in other studies in individual patients (*41*). Furthermore, the pro- or antitumorigenic effects of WGD may be context dependent (*42*–*44*), where WGD is associated with tumorigenesis by increasing aneuploidy (*45*–*47*), but may also activate cellular stress mechanisms including the p53 and Hippo pathways, as well as immune surveillance (*45*, *48*, *49*). Prior work has suggested that tumors with WGD may have unique vulnerabilities (*50*), but the mechanisms underlying the observation that WGD tumors are associated with ICB response (e.g., neoantigen presentation and increase in immunogenicity) are unclear. Our observation that timing of WGD, as measured by SNV multiplicity ratio, may be associated with outlier resistance to ICB suggests that the increased vulnerability to ICB occurs later in WGD tumors. Our results suggest that SNV multiplicity should be evaluated together with WGD and aneuploidy in future studies of biomarkers of therapy response.

We found that genomic heterogeneity positively correlates with COSMIC mutational signature 3, which is associated with defective homologous recombination-based DNA damage repair, and negatively correlates with the proportion of mutations attributed to UV signature (COSMIC Signature 7). This correlation helps explain why acral, mucosal, and uveal melanoma samples, which are typically non–sun-exposed, exhibit high genomic heterogeneity. This suggests an interesting evolutionary hypothesis: After the UV-induced ancestral melanoma clone, subclones driving genomic heterogeneity arise from different mutational processes.

Our data suggests that intratumoral genomic heterogeneity is specifically predictive of response and survival in an ICB therapy setting, while ploidy is also prognostic of worse outcomes (i.e., poor biology) even in a nontargeted or immunotherapy-treated setting. This suggests that incorporation of genomic markers such as ploidy may improve survival stratification and clinical staging and should be evaluated further [potentially in conjunction with other machine learning approaches (*51*)].

We observed that in an unbiased feature selection analysis, a recent transcriptomic signature of TLSs (*28*), but not other immune signatures including IFN-γ, added additional predictive value to genomic heterogeneity and ploidy, suggesting potential independent features that could be part of a combined biomarker using different data modalities.

We also found that a recently described melanocytic tumor state signature (*26*) is associated with intrinsic resistance to aPD-1 ICB in our cohort. This observation is unexpected because, independently from treatment, multiple studies have described a melanocytic state as less aggressive compared to dedifferentiated states such as mesenchymal-like or neural crest stem-like phenotype (*26*, *41*, *52*). In addition, no association was identified between the melanocytic state and an existing immune response (evaluating several immune signatures from the bulk RNA-seq). More in-depth study, using single-cell and spatial data, will be needed to further dissect this association.

Our approach of devising biomarkers, centered on optimizing specificity and precision, translates clinically into higher confidence in predictions within a narrower patient subset, potentially enhancing clinical applicability and acceptance. By design, we are tolerating reduced sensitivity (i.e., identification of all intrinsically resistant patients) for increased PPV of the predicted resistant patients. Our model predicted intrinsic resistance in ~20% of the entire cohort, with 90% PPV, and validated in a small independent cohort (five of five patients correctly predicted to have intrinsic resistance). We further asked whether our model simply replicates known genomic or clinical features of poor prognosis disease and response to ICB and found that our predictions were independent of known and nominated features and clinical nomograms, suggesting the independent utility of these predictions. Furthermore, application of our model in a small cohort of combination aPD-1/aCTLA-4 ICB–treated patients shows response in a notable subset (three of seven, 43%) of patients predicted to have intrinsic resistance to aPD-1 ICB, suggesting that these are indeed patients who would disproportionately benefit from combination therapy in the front-line setting. While not the primary objective of this study, the importance of optimized treatment selection is underscored by mixed results from cost-effectiveness analyses of nivolumab-ipilimumab combination therapy compared with nivolumab monotherapy where biomarkers to guide therapy choice would optimize outcomes (*53*).

There remain several limitations to this study. First, our independent validation cohorts were relatively small (in part because of careful curation of ICB-naïve tumor samples). Validation in larger cohorts is necessary, although our findings have been robust in every cohort so far. Second, our assays are based on biopsies of single lesions at a single point in time, which multiple studies (*54*, *55*) have demonstrated may not be accurate representations of tumor genomic heterogeneity even within the same lesion and differences in biopsy sites may bias our estimates. However, within our limited data, we do not observe consistent differences between genomic heterogeneity and ploidy between biopsy sites (fig. S25), and our analysis suggest robustness of our approach even without explicitly accounting for these differences. Third, the specific biological mechanisms underpinning the association of intratumoral heterogeneity and ploidy with ICB response (and prognosis) are unclear and represent important future research directions. Fourth, limiting clinical actionability, intratumoral heterogeneity and ploidy are estimated here using WES of matched tumor and normal tissue and associated analytics, which are not standardized or routinely available clinically. Standardized assessments of these genomic metrics (*56*) remain to be developed using clinically validated assays in prospective settings, although our preliminary results here suggest that the gene panels in three different clinical TNGS may allow for reasonable estimates of genomic heterogeneity for a subset of patients with higher TMB and that paired tumor-normal TNGS allow estimation of tumor ploidy. In addition, we have found our results to be robust using a different automated tool (*57*) to infer tumor heterogeneity and ploidy (fig. S5), suggesting the potential feasibility of this approach.

Together, we have demonstrated genomic heterogeneity and ploidy as robust predictors of intrinsic resistance to aPD-1 ICB in metastatic melanoma, elucidated the predictive versus prognostic role of these factors, conceived an optimized approach to building clinically pertinent predictive models, and crafted and validated a predictive model that accurately identifies patients with intrinsic resistance to aPD-1 ICB. This sets the stage for prospective studies to bring these insights into clinical practice, constituting a pivotal stride in the advancement and application of molecular biomarkers in precision oncology.

MATERIALS AND METHODS

Study design

Patients with metastatic melanoma treated with immune checkpoint blockade were identified from published work (*14*, *33*) and completed

clinical trials (BMS CheckMate-038 and CheckMate-064). We included only samples without prior exposure to ipilimumab, with WES data of the paired tumor and normal tissue obtained before PD-1 blockade. Clinicopathological and demographic data were obtained from (*14*), from BMS for the two clinical trials, and for the validation cohort from (*33*). Data are shown in Fig. 1 and in table S1. The BOR to aPD-1 ICB was only available for a subgroup of the patients included in (*33*) and was not available for the combination immunotherapy–treated ("combo") cohort. The analysis was performed by defining responders as patients achieving CR or PR as BOR; patients showing PD as BOR were instead defined as progressors. To understand whether intrinsic resistant patients to aPD-1 could benefit from the combo ICB, we also included a previously unpublished internal cohort of combo-treated samples from 13 patients. For the combo cohort, for which the BOR was not available, we defined patients that progressed in the first 6 months of treatment as progressors and compared them versus patients with PFS > 6 months. The definition of OS and PFS was from the initiation of ICB and sample collection as described in their respective studies.

This retrospective study and associated informed consent procedures were approved by the central Ethics Committee (EC) of the University Hospital Essen (12-5152-BO and 11-4715) and of Dana Farber Cancer Institute (IRB 05-042). Approval by the local EC was obtained by investigators if required by local regulations.

Quality control and variant calling

Samples from the BMS and (*33*) cohorts were reanalyzed with the Broad Institute CGA pipeline (*58*–*68*) using the TERRA platform, adopting the same quality control filters used for (*14*). In particular, quality control cutoffs were as follows: mean target coverage, >50× (tumor) and >30× (normal); cross contamination of sample estimation (ContEst), <5%; tumor purity, ≥10%, and DeTiN ≤ 20% TiN. A power filter combining coverage and tumor purity was applied as described (e.g., minimum 80% power to detect clonal mutations) in (*14*). Three samples were excluded for low purity and two samples for low power.

MuTect2 (*58*) was used to identify somatic SNVs in targeted exons, with computational filtering of artifacts introduced by DNA oxidation during sequencing or formalin-fixed paraffin embedded (FFPE)–based DNA extraction using a filter-based method (*61*). Subsequently, Strelka (*60*) was used to identify small insertions or deletions. Last, Oncotator (*68*) was used to annotate the identified alterations.

Ploidy, purity, and heterogeneity estimation

Absolute was used for the estimation of ploidy and purity and for the CCF estimation of individual mutations (*65*). For each sample, the optimal solution (purity and ploidy) was manually selected among the local solutions. Heterogeneity was computed as the proportion of the subclonal mutations, with a mutation defined as subclonal if the CCF was lower than 0.8. To support the cutoff of 0.8 for CCF, we have performed a sensitivity analysis (fig. S4), demonstrating that the heterogeneity stratification was maintained even when different cutoff values were used.

For TCGA samples, ploidy and heterogeneity were taken from (*19*) [which used FACETS (*57*) to estimate purity, ploidy, and individual mutation CCF]. For the MSK-IMPACT TNGS, the values of FACETS for purity, ploidy, and individual mutation CCF were obtained from (*6*).

SNV multiplicity and the time of WGD

The SNV multiplicity for each SNV, representing the number of copies of the SNV per cancer cell, was estimated using tumor purity and the estimated copy number state at the SNV site (q_{hat}) from ABSOLUTE (*65*) to estimate the expected variant allele fraction associated with a multiplicity of 1

$$SNV\_multiplicity\_1\_af = \frac{purity}{\left[\left(purity \times q_{\text{hat}}\right) + 2\left(1 - purity\right)\right]} \quad (1)$$

Then, SNV multiplicity was estimated using the observed tumor variant allele fraction (*tumor_f*) and the expected variant allele fraction for a multiplicity of 1

$$SNV\_multiplicity = \frac{tumor\_f}{SNV\_multiplicity\_1\_af} \quad (2)$$

We then assigned each SNV to either multiplicity 1 or 2 on the basis of a cutoff according to the distribution of the SNVs, selecting the lowest point in the histogram between the two modes of multiplicity at 1 and 2 in each individual sample (table S1). For each sample, the ratio of SNV multiplicity 2:1 alterations was used as a metric of time since the WGD event; patients with a recent WGD are characterized by high SNV multiplicity 2:1 ratio (*17*, *18*). In the modified logistic regression model, the SNV multiplicity, because it is a feature of only the WGD samples, was included as

$$\begin{aligned} SNV\ multiplicity\ score &= WGD \\ &+ WGD \times SNV\_multiplicity\_2\_to\_1\_ratio \end{aligned} \quad (3)$$

where WGD is 0 or 1, 1 for the samples with one or more WGD events.

Predictive model generation

To develop an interpretable predictive model, we focused on two model types: a logistic regression and a decision tree model. Both the models were based on just two features: heterogeneity and ploidy. To further refine our model, we performed a feature selection procedure, incorporating recently described signatures and models from (*69*), as well as different definitions of ploidy. We conducted an exhaustive forward greedy procedure using 10-fold cross-validation, selecting the features with the highest average AUC and the lowest BIC. This procedure was performed both for the subset with paired WES and RNA-seq (n = 108 with 10-fold cross-validation) and for the entire cohort. The model was trained to predict PD as the best RECIST response versus nPD rather than responder versus progressor to better reflect the real-world setting where all outcomes (PD, SD, MR, PR, and CR) are possible. We also evaluated the prediction accuracy of a logistic regression model including the SNV multiplicity as additional feature. For the standard decision tree model, we used default complexity, method="class", and to avoid overfitting, we used the value of 10 as the minimum number of samples included in the leaf. The modified decision tree model to optimize precision was obtained by increasing the relative weight of nPD samples versus PD samples in a fourfold cross-validation procedure repeated 10 times (using R package caret v 6.0.93). The choice of relative weight (nPD = 2) for the final model was selected for a tradeoff between increased precision or PPV (elbow method) and decreased sensitivity (fig. S26). The models were implemented in R version 4.2.0 using the packages stats (v 4.2.0) and rpart (v 4.1.19); for the confusion matrix and the metrics of the models, the R package caret was used. To estimate the cross-validation

AUC of the logistic regression model, we used k-fold cross-validation using $k = 10$ (splitting the dataset into k-subsets, training on $k - 1$ subsets, and calculating AUC on the holdout subset) and calculated the mean cross-validation AUC and standard deviations. Cross-validation scores were calculated using the cross_val_score function from the Python (v3) sklearn (v 1.0.2) package.

TCGA analysis

The TCGA data were obtained from (*19*). Heterogeneity was calculated using the same cutoff used for the ABSOLUTE analysis (CCF > 0.8 defined clonal mutations). Samples were initially divided into primary ($n = 61$) and metastatic ($n = 392$) samples to compare heterogeneity and ploidy; subsequent analyses focused on the metastatic lesions with OS data ($n = 381$).

Transcriptomic analysis

The methods used for sample collection, sequencing, and quality control have been described in previous work (*14*). For a subset of the samples included in the discovery cohort, bulk RNA-seq was available ($n = 108$). Only transcriptomes from tumors whose WES also passed quality control were included. To evaluate the role of IFN-γ, we used ssGSEA and signature gene sets: IFN-γ and IFN-γ related from (*15*); for the HALLMARK_INTERFERON_GAMMA_RESPONSE (*70*), we compared progressors and responders in the three cohorts used. The analysis was implemented in R using the package GSVA (v 1.44.0) (*71*) and msigdbr (v7.5.1) (*72*).

Tumor states were evaluated always using gene set enrichment analysis; the tumor states evaluated were obtained from (*26*, *27*). Bulk deconvolution was performed with BayesPrism (*73*), and for the tumor compartment, the signatures from Pozniac and Tirosh have been evaluated and compared between PD and nPD.

Survival analysis

The survival outcome of patients receiving aPD-1 was evaluated with Kaplan-Meier survival analysis. The significance of the difference in survival outcome between the patients predicted as PD [stratified by the P(PD) > 50% for the logistic regression] was assessed using a two-sided log-rank test from the survival R package. We performed this test for both OS and PFS. CheckMate-064 was a trial of sequential therapy with nivolumab and ipilimumab; therefore, patients from this trial ($n = 13$ with first-line aPD-1 ICB) were only used to identify intrinsic resistance (PD at the first restaging scan) and were excluded for the survival analysis. For the survival analysis, the cohort evaluated is $n = 111$ patients with metastatic melanoma. The impact of clinical and molecular features on OS and PFS was also tested using univariate and multivariate Cox proportional hazards model using R version 4.2.0 and the packages survival (v 3.3.1) and survminer (v 0.4.9).

Statistics and reproducibility

Statistical analyses were performed using the stats R package for R version 4.2.0. Reported P values represent nominal P values. Two primary response comparisons were made: (i) responders (defined as having CR or PR as the best RECIST response) versus progressors (defined as having PD as the best RECIST response) and (ii) progressors (PD as the best RECIST response) versus nonprogressors (nPD as best RECIST response). For the comparison between continuous clinical and molecular features, the Mann-Whitney test was used. For association of binary variables, Fisher's exact test was used. All statistical tests performed were two sided. For pairwise correlations, Spearman correlation was used.

Supplementary Materials

The PDF file includes:
Figs. S1 to S26
Legends for tables S1 to S5

Other Supplementary Material for this manuscript includes the following:
Tables S1 to S5

REFERENCES AND NOTES

1. F. S. Hodi, S. J. O'Day, D. F. McDermott, R. W. Weber, J. A. Sosman, J. B. Haanen, R. Gonzalez, C. Robert, D. Schadendorf, J. C. Hassel, W. Akerley, A. J. M. van den Eertwegh, J. Lutzky, P. Lorigan, J. M. Vaubel, G. P. Linette, D. Hogg, C. H. Ottensmeier, C. Lebbé, C. Peschel, I. Quirt, J. I. Clark, J. D. Wolchok, J. S. Weber, J. Tian, M. J. Yellin, G. M. Nichol, A. Hoos, W. J. Urba, Improved survival with ipilimumab in patients with metastatic melanoma. *N. Engl. J. Med.* **363**, 711–723 (2010).
2. C. Robert, L. Thomas, I. Bondarenko, S. O'Day, J. Weber, C. Garbe, C. Lebbe, J.-F. Baurain, A. Testori, J.-J. Grob, N. Davidson, J. Richards, M. Maio, A. Hauschild, W. H. Miller, P. Gascon, M. Lotem, K. Harmankaya, R. Ibrahim, S. Francis, T.-T. Chen, R. Humphrey, A. Hoos, J. D. Wolchok, Ipilimumab plus dacarbazine for previously untreated metastatic melanoma. *N. Engl. J. Med.* **364**, 2517–2526 (2011).
3. R. R. Munhoz, M. A. Postow, Clinical development of PD-1 in advanced melanoma. *Cancer J.* **24**, 7–14 (2018).
4. J. Larkin, V. Chiarion-Sileni, R. Gonzalez, J.-J. Grob, P. Rutkowski, C. D. Lao, C. L. Cowey, D. Schadendorf, J. Wagstaff, R. Dummer, P. F. Ferrucci, M. Smylie, D. Hogg, A. Hill, I. Márquez-Rodas, J. Haanen, M. Guidoboni, M. Maio, P. Schöffski, M. S. Carlino, C. Lebbé, G. McArthur, P. A. Ascierto, G. A. Daniels, G. V. Long, L. Bastholt, J. I. Rizzo, A. Balogh, A. Moshyk, F. S. Hodi, J. D. Wolchok, Five-year survival with combined nivolumab and ipilimumab in advanced melanoma. *N. Engl. J. Med.* **381**, 1535–1546 (2019).
5. H. A. Tawbi, D. Schadendorf, E. J. Lipson, P. A. Ascierto, L. Matamala, E. Castillo Gutiérrez, P. Rutkowski, H. J. Gogas, C. D. Lao, J. J. De Menezes, S. Dalle, A. Arance, J.-J. Grob, S. Srivastava, M. Abaskharoun, M. Hamilton, S. Keidel, K. L. Simonsen, A. M. Sobiesk, B. Li, F. S. Hodi, G. V. Long, Relatlimab and nivolumab versus nivolumab in untreated advanced melanoma. *N. Engl. J. Med.* **386**, 24–34 (2022).
6. R. M. Samstein, C.-H. Lee, A. N. Shoushtari, M. D. Hellmann, R. Shen, Y. Y. Janjigian, D. A. Barron, A. Zehir, E. J. Jordan, A. Omuro, T. J. Kaley, S. M. Kendall, R. J. Motzer, A. A. Hakimi, M. H. Voss, P. Russo, J. Rosenberg, G. Iyer, B. H. Bochner, D. F. Bajorin, H. A. Al-Ahmadie, J. E. Chaft, C. M. Rudin, G. J. Riely, S. Baxi, A. L. Ho, R. J. Wong, D. G. Pfister, J. D. Wolchok, C. A. Barker, P. H. Gutin, C. W. Brennan, V. Tabar, I. K. Mellinghoff, L. M. DeAngelis, C. E. Ariyan, N. Lee, W. D. Tap, M. M. Gounder, S. P. D'Angelo, L. Saltz, Z. K. Stadler, H. I. Scher, J. Baselga, P. Razavi, C. A. Klebanoff, R. Yaeger, N. H. Segal, G. Y. Ku, R. P. DeMatteo, M. Ladanyi, N. A. Rizvi, M. F. Berger, N. Riaz, D. B. Solit, T. A. Chan, L. G. T. Morris, Tumor mutational load predicts survival after immunotherapy across multiple cancer types. *Nat. Genet.* **51**, 202–206 (2019).
7. A. Snyder, V. Makarov, T. Merghoub, J. Yuan, J. M. Zaretsky, A. Desrichard, L. A. Walsh, M. A. Postow, P. Wong, T. S. Ho, T. J. Hollmann, C. Bruggeman, K. Kannan, Y. Li, C. Elipenahli, C. Liu, C. T. Harbison, L. Wang, A. Ribas, J. D. Wolchok, T. A. Chan, Genetic basis for clinical response to CTLA-4 blockade in melanoma. *N. Engl. J. Med.* **371**, 2189–2199 (2014).
8. N. A. Rizvi, M. D. Hellmann, A. Snyder, P. Kvistborg, V. Makarov, J. J. Havel, W. Lee, J. Yuan, P. Wong, T. S. Ho, M. L. Miller, N. Rekhtman, A. L. Moreira, F. Ibrahim, C. Bruggeman, B. Gasmi, R. Zappasodi, Y. Maeda, C. Sander, E. B. Garon, T. Merghoub, J. D. Wolchok, T. N. Schumacher, T. A. Chan, Mutational landscape determines sensitivity to PD-1 blockade in non-small cell lung cancer. *Science* **348**, 124–128 (2015).
9. E. M. Van Allen, D. Miao, B. Schilling, S. A. Shukla, C. Blank, L. Zimmer, A. Sucker, U. Hillen, M. H. G. Foppen, S. M. Goldinger, J. Utikal, J. C. Hassel, B. Weide, K. C. Kaehler, C. Loquai, P. Mohr, R. Gutzmer, R. Dummer, S. Gabriel, C. J. Wu, D. Schadendorf, L. A. Garraway, Genomic correlates of response to CTLA-4 blockade in metastatic melanoma. *Science* **350**, 207–211 (2015).
10. R. Cristescu, R. Mogg, M. Ayers, A. Albright, E. Murphy, J. Yearley, X. Sher, X. Q. Liu, H. Lu, M. Nebozhyn, C. Zhang, J. K. Lunceford, A. Joe, J. Cheng, A. L. Webber, N. Ibrahim, E. R. Plimack, P. A. Ott, T. Y. Seiwert, A. Ribas, T. K. McClanahan, J. E. Tomassini, A. Loboda, D. Kaufman, Pan-tumor genomic biomarkers for PD-1 checkpoint blockade–based immunotherapy. *Science* **362**, eaar3593 (2018).
11. J. M. Zaretsky, A. Garcia-Diaz, D. S. Shin, H. Escuin-Ordinas, W. Hugo, S. Hu-Lieskovan, D. Y. Torrejon, G. Abril-Rodriguez, S. Sandoval, L. Barthly, J. Saco, B. H. Moreno, R. Mezzadra, B. Chmielowski, K. Ruchalski, I. P. Shintaku, P. J. Sanchez, C. Puig-Saus,

G. Cherry, E. Seja, X. Kong, J. Pang, B. Berent-Maoz, B. Comin-Anduix, T. G. Graeber, P. C. Tumeh, T. N. M. Schumacher, R. S. Lo, A. Ribas, Mutations associated with acquired resistance to PD-1 blockade in melanoma. *N. Engl. J. Med.* **375**, 819–829 (2016).
12. M. Sade-Feldman, Y. J. Jiao, J. H. Chen, M. S. Rooney, M. Barzily-Rokni, J.-P. Eliane, S. L. Bjorgaard, M. R. Hammond, H. Vitzthum, S. M. Blackmon, D. T. Frederick, M. Hazar-Rethinam, B. A. Nadres, E. E. Van Seventer, S. A. Shukla, K. Yizhak, J. P. Ray, D. Rosebrock, D. Livitz, V. Adalsteinsson, G. Getz, L. M. Duncan, B. Li, R. B. Corcoran, D. P. Lawrence, A. Stemmer-Rachamimov, G. M. Boland, D. A. Landau, K. T. Flaherty, R. J. Sullivan, N. Hacohen, Resistance to checkpoint blockade therapy through inactivation of antigen presentation. *Nat. Commun.* **8**, 1136 (2017).
13. J. Gao, L. Z. Shi, H. Zhao, J. Chen, L. Xiong, Q. He, T. Chen, J. Roszik, C. Bernatchez, S. E. Woodman, P.-L. Chen, P. Hwu, J. P. Allison, A. Futreal, J. A. Wargo, P. Sharma, Loss of IFN-γ pathway genes in tumor cells as a mechanism of resistance to anti-CTLA-4 therapy. *Cell* **167**, 397–404.e9 (2016).
14. D. Liu, B. Schilling, D. Liu, A. Sucker, E. Livingstone, L. Jerby-Arnon, L. Zimmer, R. Gutzmer, I. Satzger, C. Loquai, S. Grabbe, N. Vokes, C. A. Margolis, J. Conway, M. X. He, H. Elmarakeby, F. Dietlein, D. Miao, A. Tracy, H. Gogas, S. M. Goldinger, J. Utikal, C. U. Blank, R. Rauschenberg, D. von Bubnoff, A. Krackhardt, B. Weide, S. Haferkamp, F. Kiecker, B. Izar, L. Garraway, A. Regev, K. Flaherty, A. Paschen, E. M. Van Allen, D. Schadendorf, Integrative molecular and clinical modeling of clinical outcomes to PD1 blockade in patients with metastatic melanoma. *Nat. Med.* **25**, 1916–1927 (2019).
15. S. J. Rodig, D. Gusenleitner, D. G. Jackson, E. Gjini, A. Giobbie-Hurder, C. Jin, H. Chang, S. B. Lovitch, C. Horak, J. S. Weber, J. L. Weirather, J. D. Wolchok, M. A. Postow, A. C. Pavlick, J. Chesney, F. S. Hodi, MHC proteins confer differential sensitivity to CTLA-4 and PD-1 blockade in untreated metastatic melanoma. *Sci. Transl. Med.* **10**, eaar3342 (2018).
16. N. Riaz, J. J. Havel, V. Makarov, A. Desrichard, W. J. Urba, J. S. Sims, F. S. Hodi, S. Martín-Algarra, R. Mandal, W. H. Sharfman, S. Bhatia, W.-J. Hwu, T. F. Gajewski, C. L. Slingluff, D. Chowell, S. M. Kendall, H. Chang, R. Shah, F. Kuo, L. G. T. Morris, J.-W. Sidhom, J. P. Schneck, C. E. Horak, N. Weinhold, T. A. Chan, Tumor and microenvironment evolution during immunotherapy with nivolumab. *Cell* **171**, 934–949.e16 (2017).
17. M. Tarabichi, A. Salcedo, A. G. Deshwar, M. Ni Leathlobhair, J. Wintersinger, D. C. Wedge, P. Van Loo, Q. D. Morris, P. C. Boutros, A practical guide to cancer subclonal reconstruction from DNA sequencing. *Nat. Methods* **18**, 144–155 (2021).
18. S. C. Dentro, I. Leshchiner, K. Haase, M. Tarabichi, J. Wintersinger, A. G. Deshwar, K. Yu, Y. Rubanova, G. Macintyre, J. Demeulemeester, I. Vázquez-García, K. Kleinheinz, D. G. Livitz, S. Malikic, N. Donmez, S. Sengupta, P. Anur, C. Jolly, M. Cmero, D. Rosebrock, S. E. Schumacher, Y. Fan, M. Fittall, R. M. Drews, X. Yao, T. B. K. Watkins, J. Lee, M. Schlesner, H. Zhu, D. J. Adams, N. McGranahan, C. Swanton, G. Getz, P. C. Boutros, M. Imielinski, R. Beroukhim, S. C. Sahinalp, Y. Ji, M. Peifer, I. Martincorena, F. Markowetz, V. Mustonen, K. Yuan, M. Gerstung, P. T. Spellman, W. Wang, Q. D. Morris, D. C. Wedge, P. Van Loo, S. C. Dentro, I. Leshchiner, M. Gerstung, C. Jolly, K. Haase, M. Tarabichi, J. Wintersinger, A. G. Deshwar, K. Yu, S. Gonzalez, Y. Rubanova, G. Macintyre, J. Demeulemeester, D. J. Adams, P. Anur, R. Beroukhim, P. C. Boutros, D. D. Bowtell, P. J. Campbell, S. Cao, E. L. Christie, M. Cmero, Y. Cun, K. J. Dawson, N. Donmez, R. M. Drews, R. Eils, Y. Fan, M. Fittall, D. W. Garsed, G. Getz, G. Ha, M. Imielinski, L. Jerman, Y. Ji, K. Kleinheinz, J. Lee, H. Lee-Six, D. G. Livitz, S. Malikic, F. Markowetz, I. Martincorena, T. J. Mitchell, V. Mustonen, L. Oesper, M. Peifer, M. Peto, B. J. Raphael, D. Rosebrock, S. C. Sahinalp, A. Salcedo, M. Schlesner, S. E. Schumacher, S. Sengupta, R. Shi, S. J. Shin, L. D. Stein, O. Spiro, I. Vázquez-García, S. Vembu, D. A. Wheeler, T.-P. Yang, X. Yao, K. Yuan, H. Zhu, W. Wang, Q. D. Morris, P. T. Spellman, D. C. Wedge, P. Van Loo, Characterizing genetic intra-tumor heterogeneity across 2,658 human cancer genomes. *Cell* **184**, 2239–2254.e39 (2021).
19. J. R. Conway, F. Dietlein, A. Taylor-Weiner, S. AlDubayan, N. Vokes, T. Keenan, B. Reardon, M. X. He, C. A. Margolis, J. L. Weirather, R. Haq, B. Schilling, F. Stephen Hodi, D. Schadendorf, D. Liu, E. M. Van Allen, Integrated molecular drivers coordinate biological and clinical states in melanoma. *Nat. Genet.* **52**, 1373–1383 (2020).
20. C. M. Bielski, A. Zehir, A. V. Penson, M. T. A. Donoghue, W. Chatila, J. Armenia, M. T. Chang, A. M. Schram, P. Jonsson, C. Bandlamudi, P. Razavi, G. Iyer, M. E. Robson, Z. K. Stadler, N. Schultz, J. Baselga, D. B. Solit, D. M. Hyman, M. F. Berger, B. S. Taylor, Genome doubling shapes the evolution and prognosis of advanced cancers. *Nat. Genet.* **50**, 1189–1195 (2018).
21. R. Newcomb, E. Dean, B. J. McKinney, J. V. Alvarez, Context-dependent effects of whole-genome duplication during mammary tumor recurrence. *Sci. Rep.* **11**, 14932 (2021).
22. S. M. Dewhurst, N. McGranahan, R. A. Burrell, A. J. Rowan, E. Grönroos, D. Endesfelder, T. Joshi, D. Mouradov, P. Gibbs, R. L. Ward, N. J. Hawkins, Z. Szallasi, O. M. Sieber, C. Swanton, Tolerance of whole-genome doubling propagates chromosomal instability and accelerates cancer genome evolution. *Cancer Discov.* **4**, 175–185 (2014).
23. F. Newell, P. A. Johansson, J. S. Wilmott, K. Nones, V. Lakis, A. L. Pritchard, S. N. Lo, R. V. Rawson, S. H. Kazakoff, A. J. Colebatch, L. T. Koufariotis, P. M. Ferguson, S. Wood, C. Leonard, M. H. Law, K. M. Brooks, N. Broit, J. M. Palmer, K. L. Couts, I. A. Vergara, G. V. Long, A. P. Barbour, O. E. Nieweg, B. Shivalingam, W. A. Robinson, J. R. Stretch, A. J. Spillane, R. P. M. Saw, K. F. Shannon, J. F. Thompson, G. J. Mann, J. V. Pearson, R. A. Scolyer, N. Waddell, N. K. Hayward, Comparative genomics provides etiologic and biological insight into melanoma subtypes. *Cancer Discov.* **12**, 2856–2879 (2022).
24. L. B. Alexandrov, J. Kim, N. J. Haradhvala, M. N. Huang, A. W. T. Ng, Y. Wu, A. Boot, K. R. Covington, D. A. Gordenin, E. N. Bergstrom, S. M. A. Islam, N. Lopez-Bigas, L. J. Klimczak, J. R. Mc Pherson, S. Morganella, R. Sabarinathan, D. A. Wheeler, V. Mustonen, PCAWG Mutational Signatures Working Group, G. Getz, S. G. Rozen, M. R. Stratton, PCAWG Consortium, The repertoire of mutational signatures in human cancer. *Nature* **578**, 94–101 (2020).
25. K. M. Campbell, M. Amouzgar, S. M. Pfeiffer, T. R. Howes, E. Medina, M. Travers, G. Steiner, J. S. Weber, J. D. Wolchok, J. Larkin, F. S. Hodi, S. Boffo, L. Salvador, D. Tenney, T. Tang, M. A. Thompson, C. N. Spencer, D. K. Wells, A. Ribas, Prior anti-CTLA-4 therapy impacts molecular characteristics associated with anti-PD-1 response in advanced melanoma. *Cancer Cell* **41**, 791–806.e4 (2023).
26. J. Pozniak, D. Pedri, E. Landeloos, Y. Van Herck, A. Antoranz, L. Vanwynsberghe, A. Nowosad, N. Roda, S. Makhzami, G. Bervoets, L. F. Maciel, C. A. Pulido-Vicuña, L. Pollaris, R. Seurinck, F. Zhao, K. Flem-Karlsen, W. Damsky, L. Chen, D. Karagianni, S. Cinque, S. Kint, K. Vandereyken, B. Rombaut, T. Voet, F. Vernaillen, W. Annaert, D. Lambrechts, V. Boecxstaens, Y. Saeys, J. Van Den Oord, F. Bosisio, P. Karras, A. H. Shain, M. Bosenberg, E. Leucci, A. Paschen, F. Rambow, O. Bechter, J.-C. Marine, A TCF4-dependent gene regulatory network confers resistance to immunotherapy in melanoma. *Cell* **187**, 166–183.e25 (2024).
27. I. Tirosh, B. Izar, S. M. Prakadan, M. H. Wadsworth II, D. Treacy, J. J. Trombetta, A. Rotem, C. Rodman, C. Lian, G. Murphy, M. Fallahi-Sichani, K. Dutton-Regester, J.-R. Lin, O. Cohen, P. Shah, D. Lu, A. S. Genshaft, T. K. Hughes, C. G. K. Ziegler, S. W. Kazer, A. Gaillard, K. E. Kolb, A.-C. Villani, C. M. Johannessen, A. Y. Andreev, E. M. V. Allen, M. Bertagnolli, P. K. Sorger, R. J. Sullivan, K. T. Flaherty, D. T. Frederick, J. Jané-Valbuena, C. H. Yoon, O. Rozenblatt-Rosen, A. K. Shalek, A. Regev, L. A. Garraway, Dissecting the multicellular ecosystem of metastatic melanoma by single-cell RNA-seq. *Science* **352**, 189–196 (2016).
28. R. Cabrita, M. Lauss, A. Sanna, M. Donia, M. Skaarup Larsen, S. Mitra, I. Johansson, B. Phung, K. Harbst, J. Vallon-Christersson, A. Van Schoiack, K. Lövgren, S. Warren, K. Jirström, H. Olsson, K. Pietras, C. Ingvar, K. Isaksson, D. Schadendorf, H. Schmidt, L. Bastholt, A. Carneiro, J. A. Wargo, I. M. Svane, G. Jönsson, Tertiary lymphoid structures improve immunotherapy and survival in melanoma. *Nature* **577**, 561–565 (2020).
29. H. A. Tawbi, P. A. Forsyth, A. Algazi, O. Hamid, F. S. Hodi, S. J. Moschos, N. I. Khushalani, K. Lewis, C. D. Lao, M. A. Postow, M. B. Atkins, M. S. Ernstoff, D. A. Reardon, I. Puzanov, R. R. Kudchadkar, R. P. Thomas, A. Tarhini, A. C. Pavlick, J. Jiang, A. Avila, S. Demelo, K. Margolin, Combined nivolumab and ipilimumab in melanoma metastatic to the brain. *N. Engl. J. Med.* **379**, 722–730 (2018).
30. G. V. Long, V. Atkinson, S. Lo, S. Sandhu, A. D. Guminski, M. P. Brown, J. S. Wilmott, J. Edwards, M. Gonzalez, R. A. Scolyer, A. M. Menzies, G. A. McArthur, Combination nivolumab and ipilimumab or nivolumab alone in melanoma brain metastases: A multicentre randomised phase 2 study. *Lancet Oncol.* **19**, 672–681 (2018).
31. E. A. T. Koch, A. Petzold, A. Wessely, E. Dippel, A. Gesierich, R. Gutzmer, J. Hassel, S. Haferkamp, B. Hohberger, K. Kähler, H. Knorr, N. Kreuzberg, U. Leiter, C. Loquai, F. Meier, M. Meissner, P. Mohr, C. Pföhler, F. Rahimi, D. Schadendorf, B. Schell, M. Schlaak, P. Terheyden, K.-M. Thoms, B. Schuler-Thurner, S. Ugurel, J. Ulrich, J. Utikal, M. Weichenthal, F. Ziller, C. Berking, M. Heppt, On Behalf Of The German Dermatologic Cooperative Oncology Group DeCOG Committee Ocular Melanoma, Immune checkpoint blockade for metastatic uveal melanoma: Patterns of response and survival according to the presence of hepatic and extrahepatic metastasis. *Cancers* **13**, 3359 (2021).
32. I. Pires da Silva, T. Ahmed, J. L. McQuade, C. A. Nebhan, J. J. Park, J. M. Versluis, P. Serra-Bellver, Y. Khan, T. Slattery, H. K. Oberoi, S. Ugurel, L. E. Haydu, R. Herbst, J. Utikal, C. Pföhler, P. Terheyden, M. Weichenthal, R. Gutzmer, P. Mohr, R. Rai, J. L. Smith, R. A. Scolyer, A. M. Arance, L. Pickering, J. Larkin, P. Lorigan, C. U. Blank, D. Schadendorf, M. A. Davies, M. S. Carlino, D. B. Johnson, G. V. Long, S. N. Lo, A. M. Menzies, Clinical models to define response and survival with anti–PD-1 antibodies alone or combined with ipilimumab in metastatic melanoma. *J. Clin. Oncol.* **40**, 1068–1080 (2022).
33. S. S. Freeman, M. Sade-Feldman, J. Kim, C. Stewart, A. L. K. Gonye, A. Ravi, M. B. Arniella, I. Gushterova, T. J. LaSalle, E. M. Blaum, K. Yizhak, D. T. Frederick, T. Sharova, I. Leshchiner, L. Elagina, O. G. Spiro, D. Livitz, D. Rosebrock, F. Aguet, J. Carrot-Zhang, G. Ha, Z. Lin, J. H. Chen, M. Barzily-Rokni, M. R. Hammond, H. C. Vitzthum von Eckstaedt, S. M. Blackmon, Y. J. Jiao, S. Gabriel, D. P. Lawrence, L. M. Duncan, A. O. Stemmer-Rachamimov, J. A. Wargo, K. T. Flaherty, R. J. Sullivan, G. M. Boland, M. Meyerson, G. Getz, N. Hacohen, Combined tumor and immune signals from genomes or transcriptomes predict outcomes of checkpoint inhibition in melanoma. *Cell Rep. Med.* **3**, 100500 (2022).
34. E. Rossi, G. Schinzari, B. A. Maiorano, G. Indellicati, A. Di Stefani, M. M. Pagliara, S. M. Fragomeni, E. V. De Luca, M. G. Sammarco, G. Garganese, J. Galli, M. A. Blasi, G. Paludetti, G. Scambia, K. Peris, G. Tortora, Efficacy of immune checkpoint inhibitors in different types of melanoma. *Hum. Vaccin. Immunother.* **17**, 4–13 (2021).
35. C. E. Meacham, S. J. Morrison, Tumour heterogeneity and cancer cell plasticity. *Nature* **501**, 328–337 (2013).
36. N. McGranahan, A. J. S. Furness, R. Rosenthal, S. Ramskov, R. Lyngaa, S. K. Saini, M. Jamal-Hanjani, G. A. Wilson, N. J. Birkbak, C. T. Hiley, T. B. K. Watkins, S. Shafi,

N. Murugaesu, R. Mitter, A. U. Akarca, J. Linares, T. Marafioti, J. Y. Henry, E. M. Van Allen, D. Miao, B. Schilling, D. Schadendorf, L. A. Garraway, V. Makarov, N. A. Rizvi, A. Snyder, M. D. Hellmann, T. Merghoub, J. D. Wolchok, S. A. Shukla, C. J. Wu, K. S. Peggs, T. A. Chan, S. R. Hadrup, S. A. Quezada, C. Swanton, Clonal neoantigens elicit T cell immunoreactivity and sensitivity to immune checkpoint blockade. *Science* **351**, 1463–1469 (2016).
37. L. G. T. Morris, N. Riaz, A. Desrichard, Y. Şenbabaoğlu, A. A. Hakimi, V. Makarov, J. S. Reis-Filho, T. A. Chan, Pan-cancer analysis of intratumor heterogeneity as a prognostic determinant of survival. *Oncotarget* **7**, 10051–10063 (2016).
38. N. Andor, T. A. Graham, M. Jansen, L. C. Xia, C. A. Aktipis, C. Petritsch, H. P. Ji, C. C. Maley, Pan-cancer analysis of the extent and consequences of intratumor heterogeneity. *Nat. Med.* **22**, 105–113 (2016).
39. Y. Wolf, O. Bartok, S. Patkar, G. B. Eli, S. Cohen, K. Litchfield, R. Levy, A. Jiménez-Sánchez, S. Trabish, J. S. Lee, H. Karathia, E. Barnea, C.-P. Day, E. Cinnamon, I. Stein, A. Solomon, L. Bitton, E. Pérez-Guijarro, T. Dubovik, S. S. Shen-Orr, M. L. Miller, G. Merlino, Y. Levin, E. Pikarsky, L. Eisenbach, A. Admon, C. Swanton, E. Ruppin, Y. Samuels, UVB-induced tumor heterogeneity diminishes immune response in melanoma. *Cell* **179**, 219–235.e21 (2019).
40. S. López, E. L. Lim, S. Horswell, K. Haase, A. Huebner, M. Dietzen, T. P. Mourikis, T. B. K. Watkins, A. Rowan, S. M. Dewhurst, N. J. Birkbak, G. A. Wilson, P. Van Loo, M. Jamal-Hanjani, TRACERx Consortium, C. Swanton, N. McGranahan, Interplay between whole-genome doubling and the accumulation of deleterious alterations in cancer evolution. *Nat. Genet.* **52**, 283–293 (2020).
41. D. Liu, J.-R. Lin, E. J. Robitschek, G. G. Kasumova, A. Heyde, A. Shi, A. Kraya, G. Zhang, T. Moll, D. T. Frederick, Y.-A. Chen, S. Wang, D. Schapiro, L.-L. Ho, K. Bi, A. Sahu, S. Mei, B. Miao, T. Sharova, C. Alvarez-Breckenridge, J. H. Stocking, T. Kim, R. Fadden, D. Lawrence, M. P. Hoang, D. P. Cahill, M. Malehmir, M. A. Nowak, P. K. Brastianos, C. G. Lian, E. Ruppin, B. Izar, M. Herlyn, E. M. Van Allen, K. Nathanson, K. T. Flaherty, R. J. Sullivan, M. Kellis, P. K. Sorger, G. M. Boland, Evolution of delayed resistance to immunotherapy in a melanoma responder. *Nat. Med.* **27**, 985–992 (2021).
42. E. M. Torres, T. Sokolsky, C. M. Tucker, L. Y. Chan, M. Boselli, M. J. Dunham, A. Amon, Effects of aneuploidy on cellular physiology and cell division in haploid yeast. *Science* **317**, 916–924 (2007).
43. B. R. Williams, V. R. Prabhu, K. E. Hunter, C. M. Glazier, C. A. Whittaker, D. E. Housman, A. Amon, Aneuploidy affects proliferation and spontaneous immortalization in mammalian cells. *Science* **322**, 703–709 (2008).
44. S. Stingele, G. Stoehr, K. Peplowska, J. Cox, M. Mann, Z. Storchova, Global analysis of genome, transcriptome and proteome reveals the response to aneuploidy in human cells. *Mol. Syst. Biol.* **8**, 608 (2012).
45. T. Fujiwara, M. Bandi, M. Nitta, E. V. Ivanova, R. T. Bronson, D. Pellman, Cytokinesis failure generating tetraploids promotes tumorigenesis in p53-null cells. *Nature* **437**, 1043–1047 (2005).
46. N. J. Ganem, S. A. Godinho, D. Pellman, A mechanism linking extra centrosomes to chromosomal instability. *Nature* **460**, 278–282 (2009).
47. L. Lv, T. Zhang, Q. Yi, Y. Huang, Z. Wang, H. Hou, H. Zhang, W. Zheng, Q. Hao, Z. Guo, H. J. Cooke, Q. Shi, Tetraploid cells from cytokinesis failure induce aneuploidy and spontaneous transformation of mouse ovarian surface epithelial cells. *Cell Cycle* **11**, 2864–2875 (2012).
48. S. Santaguida, A. Richardson, D. R. Iyer, O. M'Saad, L. Zasadil, K. A. Knouse, Y. L. Wong, N. Rhind, A. Desai, A. Amon, Chromosome mis-segregation generates cell-cycle-arrested cells with complex karyotypes that are eliminated by the immune system. *Dev. Cell* **41**, 638–651.e5 (2017).
49. T. Davoli, T. de Lange, Telomere-driven tetraploidization occurs in human cells undergoing crisis and promotes transformation of mouse cells. *Cancer Cell* **21**, 765–776 (2012).
50. R. J. Quinton, A. DiDomizio, M. A. Vittoria, K. Kotýnková, C. J. Ticas, S. Patel, Y. Koga, J. Vakhshoorzadeh, N. Hermance, T. S. Kuroda, N. Parulekar, A. M. Taylor, A. L. Manning, J. D. Campbell, N. J. Ganem, Whole-genome doubling confers unique genetic vulnerabilities on tumour cells. *Nature* **590**, 492–497 (2021).
51. G. Wan, N. Nguyen, F. Liu, M. S. DeSimone, B. W. Leung, A. Rajeh, M. R. Collier, M. S. Choi, M. Amadife, K. Tang, S. Zhang, J. S. Phillipps, R. Jairath, N. A. Alexander, Y. Hua, M. Jiao, W. Chen, D. Ho, S. Duey, I. B. Németh, G. Marko-Varga, J. G. Valdés, D. Liu, G. M. Boland, A. Gusev, P. K. Sorger, K.-H. Yu, Y. R. Semenov, Prediction of early-stage melanoma recurrence using clinical and histopathologic features. *NPJ Precis. Onc.* **6**, 79 (2022).
52. F. Rambow, A. Rogiers, O. Marin-Bejar, S. Aibar, J. Femel, M. Dewaele, P. Karras, D. Brown, Y. H. Chang, M. Debiec-Rychter, C. Adriaens, E. Radaelli, P. Wolter, O. Bechter, R. Dummer, M. Levesque, A. Piris, D. T. Frederick, G. Boland, K. T. Flaherty, J. Van Den Oord, T. Voet, S. Aerts, A. W. Lund, J.-C. Marine, Toward minimal residual disease-directed therapy in melanoma. *Cell* **174**, 843–855.e19 (2018).
53. A. Oh, D. M. Tran, L. C. McDowell, D. Keyvani, J. A. Barcelon, O. Merino, L. Wilson, Cost-effectiveness of nivolumab-ipilimumab combination therapy compared with monotherapy for first-line treatment of metastatic melanoma in the United States. *J. Manag. Care Spec. Pharm.* **23**, 653–664 (2017).
54. M. Gerlinger, A. J. Rowan, S. Horswell, J. Larkin, D. Endesfelder, E. Gronroos, P. Martinez, N. Matthews, A. Stewart, P. Tarpey, I. Varela, B. Phillimore, S. Begum, N. Q. McDonald, A. Butler, D. Jones, K. Raine, C. Latimer, C. R. Santos, M. Nohadani, A. C. Eklund, B. Spencer-Dene, G. Clark, L. Pickering, G. Stamp, M. Gore, Z. Szallasi, J. Downward, P. A. Futreal, C. Swanton, Intratumor heterogeneity and branched evolution revealed by multiregion sequencing. *N. Engl. J. Med.* **366**, 883–892 (2012).
55. J. Schiantarelli, T. Pappa, J. Conway, J. Crowdis, B. Reardon, F. Dietlein, J. Huang, D. Stanizzi, E. Carey, A. Bosma-Moody, A. Imamovic, S. Han, S. Camp, E. Kofman, E. Shannon, J. A. Barletta, M. X. He, D. Liu, J. Park, J. H. Lorch, E. M. Van Allen, Mutational footprint of platinum chemotherapy in a secondary thyroid cancer. *JCO Precis. Oncol.* **6**, e2200183 (2022).
56. N. I. Vokes, D. Liu, B. Ricciuti, E. Jimenez-Aguilar, H. Rizvi, F. Dietlein, M. X. He, C. A. Margolis, H. A. Elmarakeby, J. Girshman, A. Adeni, F. Sanchez-Vega, N. Schultz, S. Dahlberg, A. Zehir, P. A. Jänne, M. Nishino, R. Umeton, L. M. Sholl, E. M. Van Allen, M. D. Hellmann, M. M. Awad, Harmonization of tumor mutational burden quantification and association with response to immune checkpoint blockade in non–small-cell lung cancer. *JCO Precis. Oncol.* **3**, 10.1200/PO.19.00171 (2019).
57. R. Shen, V. E. Seshan, FACETS: Allele-specific copy number and clonal heterogeneity analysis tool for high-throughput DNA sequencing. *Nucleic Acids Res.* **44**, e131 (2016).
58. K. Cibulskis, M. S. Lawrence, S. L. Carter, A. Sivachenko, D. Jaffe, C. Sougnez, S. Gabriel, M. Meyerson, E. S. Lander, G. Getz, Sensitive detection of somatic point mutations in impure and heterogeneous cancer samples. *Nat. Biotechnol.* **31**, 213–219 (2013).
59. K. Cibulskis, A. McKenna, T. Fennell, E. Banks, M. DePristo, G. Getz, ContEst: Estimating cross-contamination of human samples in next-generation sequencing data. *Bioinformatics* **27**, 2601–2602 (2011).
60. C. T. Saunders, W. S. W. Wong, S. Swamy, J. Becq, L. J. Murray, R. K. Cheetham, Strelka: Accurate somatic small-variant calling from sequenced tumor–normal sample pairs. *Bioinformatics* **28**, 1811–1817 (2012).
61. M. Costello, T. J. Pugh, T. J. Fennell, C. Stewart, L. Lichtenstein, J. C. Meldrim, J. L. Fostel, D. C. Friedrich, D. Perrin, D. Dionne, S. Kim, S. B. Gabriel, E. S. Lander, S. Fisher, G. Getz, Discovery and characterization of artifactual mutations in deep coverage targeted capture sequencing data due to oxidative DNA damage during sample preparation. *Nucleic Acids Res.* **41**, e67 (2013).
62. A. Taylor-Weiner, C. Stewart, T. Giordano, M. Miller, M. Rosenberg, A. Macbeth, N. Lennon, E. Rheinbay, D.-A. Landau, C. J. Wu, G. Getz, DeTiN: Overcoming tumor-in-normal contamination. *Nat. Methods* **15**, 531–534 (2018).
63. D. A. Landau, S. L. Carter, P. Stojanov, A. McKenna, K. Stevenson, M. S. Lawrence, C. Sougnez, C. Stewart, A. Sivachenko, L. Wang, Y. Wan, W. Zhang, S. A. Shukla, A. Vartanov, S. M. Fernandes, G. Saksena, K. Cibulskis, B. Tesar, S. Gabriel, N. Hacohen, M. Meyerson, E. S. Lander, D. Neuberg, J. R. Brown, G. Getz, C. J. Wu, Evolution and impact of subclonal mutations in chronic lymphocytic leukemia. *Cell* **152**, 714–726 (2013).
64. M. S. Lawrence, P. Stojanov, C. H. Mermel, J. T. Robinson, L. A. Garraway, T. R. Golub, M. Meyerson, S. B. Gabriel, E. S. Lander, G. Getz, Discovery and saturation analysis of cancer genes across 21 tumour types. *Nature* **505**, 495–501 (2014).
65. S. L. Carter, K. Cibulskis, E. Helman, A. McKenna, H. Shen, T. Zack, P. W. Laird, R. C. Onofrio, W. Winckler, B. A. Weir, R. Beroukhim, D. Pellman, D. A. Levine, E. S. Lander, M. Meyerson, G. Getz, Absolute quantification of somatic DNA alterations in human cancer. *Nat. Biotechnol.* **30**, 413–421 (2012).
66. A. McKenna, M. Hanna, E. Banks, A. Sivachenko, K. Cibulskis, A. Kernytsky, K. Garimella, D. Altshuler, S. Gabriel, M. Daly, M. A. DePristo, The genome analysis toolkit: A MapReduce framework for analyzing next-generation DNA sequencing data. *Genome Res.* **20**, 1297–1303 (2010).
67. W. McLaren, L. Gil, S. E. Hunt, H. S. Riat, G. R. S. Ritchie, A. Thormann, P. Flicek, F. Cunningham, The Ensembl variant effect predictor. *Genome Biol.* **17**, 122 (2016).
68. A. H. Ramos, L. Lichtenstein, M. Gupta, M. S. Lawrence, T. J. Pugh, G. Saksena, M. Meyerson, G. Getz, Oncotator: Cancer variant annotation tool. *Hum. Mutat.* **36**, E2423–E2429 (2015).
69. M. Mason, Ó. Lapuente-Santana, A. S. Halkola, W. Wang, R. Mall, X. Xiao, J. Kaufman, J. Fu, J. Pfeil, J. Banerjee, V. Chung, H. Chang, S. D. Chasalow, H. Y. Lin, R. Chai, T. Yu, F. Finotello, T. Mirtti, M. I. Mäyränpää, J. Bao, E. W. Verschuren, E. I. Ahmed, M. Ceccarelli, L. D. Miller, G. Monaco, W. R. L. Hendrickx, S. Sherif, L. Yang, M. Tang, S. S. Gu, W. Zhang, Y. Zhang, Z. Zeng, A. Das Sahu, Y. Liu, W. Yang, D. Bedognetti, J. Tang, F. Eduati, T. D. Laajala, W. J. Geese, J. Guinney, J. D. Szustakowski, B. G. Vincent, D. P. Carbone, A community challenge to predict clinical outcomes after immune checkpoint blockade in non-small cell lung cancer. *J. Transl. Med.* **22**, 190 (2024).
70. A. Liberzon, C. Birger, H. Thorvaldsdóttir, M. Ghandi, J. P. Mesirov, P. Tamayo, The Molecular Signatures Database hallmark gene set collection. *Cell Syst.* **1**, 417–425 (2015).
71. S. Hänzelmann, R. Castelo, J. Guinney, GSVA: Gene set variation analysis for microarray and RNA-seq data. *BMC Bioinformatics* **14**, 7 (2013).
72. A. Subramanian, P. Tamayo, V. K. Mootha, S. Mukherjee, B. L. Ebert, M. A. Gillette, A. Paulovich, S. L. Pomeroy, T. R. Golub, E. S. Lander, J. P. Mesirov, Gene set enrichment analysis: A knowledge-based approach for interpreting genome-wide expression profiles. *Proc. Natl. Acad. Sci. U.S.A.* **102**, 15545–15550 (2005).

73. T. Chu, Z. Wang, D. Pe'er, C. G. Danko, Cell type and gene expression deconvolution with BayesPrism enables Bayesian integrative analysis across bulk and single-cell RNA sequencing in oncology. *Nat. Cancer* **3**, 505–517 (2022); https://doi.org/10.1038/s43018-022-00356-3.

Acknowledgments: This work was supported, in part, by the NIH and the Doris Duke Charitable Foundation. This work was funded by Bristol Myers Squibb through its International Immuno-Oncology Network. G.T. was supported by an American-Italian Cancer Foundation Post-Doctoral Research Fellowship. The results presented here are, in part, based on data generated by TCGA Research Network. The authors acknowledge the research support from the Adelson Medical Research Foundation (AMRF; to G.M.B.), the Patricia K. Donahoe Award from the Huiying Foundation (to G.M.B.), and the Emma and Bill Roberts MGH Research Scholar Award (to G.M.B.). **Funding:** NIH grant K08CA234458 (D.L.), Bristol Myers Squibb grant II-ON TM-231(D.L.), Doris Duke Charitable Foundation Clinical Scientist Training Program (D.L.), and American-Italian Cancer Foundation Post-Doctoral Research Fellowship (G.T.). **Author contributions:** Conceptualization: G.T., D.L., D.S., E.M.V.A., G.M.B., N.I.V., A.G.-H., W.G., A.Z., S.M., C.J.W., Y.S., S.S., M.M.H., M.G., K.T.F., B.S., and F.S.H. Data curation: G.T., N.I.V., G.M.B., M.P.M., D.S., L.G.T.M., A.Z., S.M., S.F., D.T.F., C.H.F., A.L., Y.S., D.L., and K.T.F. Methodology: G.T., D.L., A.G.-H., W.G., A.W., D.S., L.G.T.M., A.Z., S.M., Y.S., S.S., E.M.V.A., M.G., C.A.R., and N.I.V. Formal analysis: G.T., C.A.R., A.W., A.G.-H., W.G., J.C., L.G.T.M., S.M., A.Y.H., C.J.W., C.H.F., T.J.A., N.I.V., Y.S., S.S., E.M.V.A., D.L., J.C.J., and M.G. Investigation: G.T., H.A.E., W.G., G.M.B., M.P.M., L.G.T.M., D.T.F., C.H.F., Y.S., M.M.H., M.G., K.T.F., E.I.B., F.S.H., and B.S. Visualization: G.T., W.G., G.M.B., L.G.T.M., T.J.A., C.H.F., D.L., J.C.J., and F.S.H. Funding acquisition: D.L., E.M.V.A., D.S., and F.S.H. Supervision: D.L., H.A.E., N.I.V., G.M.B., M.P.M., D.S., F.S.H., and C.J.W. Writing (original draft): G.T., D.L., G.M.B., and F.S.H. Writing (review and editing): G.T., H.A.E., N.I.V., A.G.-H., G.M.B., R.H., J.P., D.S., A.R., L.Z., T.J.A., S.S., M.M.H., D.L., F.S.H., and B.S. Resources: G.T., B.R., G.M.B., J.P., D.S., L.G.T.M., A.R., L.Z., C.J.W., E.L., Y.S., E.M.V.A., D.L., K.T.F., E.I.B., F.S.H., and B.S. Validation: G.T., K.Z., G.M.B., D.S., J.C., L.G.T.M., S.M., A.R., T.J.A., C.H.F., A.L., Y.S., E.M.V.A., D.L., J.C.J., and M.G. Software: G.T., W.G., A.W., L.G.T.M., S.M., A.Y.H., T.J.A., C.H.F., Y.S., and J.C.J. Project administration: D.L., G.M.B., M.P.M., D.S., L.G.T.M., and F.S.H. **Competing interests:** G.M.B. has sponsored research agreements through her institution with Olink Proteomics, Teiko Bio, InterVenn Biosciences, and Palleon Pharmaceuticals. She served on advisory boards for Iovance, Merck, Moderna, Nektar Therapeutics, Novartis, and Ankyra Therapeutics. She consults for Merck, InterVenn Biosciences, Iovance, and Ankyra Therapeutics. She holds equity in Ankyra Therapeutics. D.S. has sponsored research agreement through his institution with Amgen, BMS, MSD, and Pfizer; consulting fees/honoraria from Philogen, InFlarX, Neracare, Merck Sharp & Dohme, Novartis, Bristol Myers Squibb, Pfizer, Pierre Fabre, Replimune, SunPharma, Daiichi Sanyo, Astra Zeneca, IQVIA, LabCorp, UltimoVacs, Seagen, Immunocore, Immatics, BioNTech, PamGene, BioAlta, Regeneron, Agenus, Erasca, Formycon, NoviGenix, CureVac, and Sanofi Travel: Pierre Fabre; participation on data safety monitoring from Immunocore, AstraZeneca, BioAlta, Daiichi Sancyo, InFlarX, and Replimune; and leadership role for EORTC-MG steering board, DeCOG steering board, NVKH chair, and CCC chair. E.I.B. serves as a consultant/advisory board member for Pfizer, Werewolf Pharma, Merck, Iovance, Sanofi, Xilio, and Novartis; clinical trial support from Lilly, Novartis, Partners Therapeutics, Genentech, and BVD. F.S.H. has receives grants and personal fees from Bristol Myers Squibb and Novartis and personal fees from Merck, Surface, Compass Therapeutics, Apricity, Bicara, Checkpoint Therapeutics, Genentech/Roche, Bioentre, Gossamer, Iovance, Catalym, Immunocore, Kairos, Rheos, Zumutor, Corner Therapeutics, Puretech, Curis, and Astra Zeneca, outside the submitted work. L.Z. served as consultant and has received honoraria from BMS, MSD, Novartis, Pierre Fabre, Sanofi, and Sunpharma and travel support from MSD, BMS, Pierre Fabre, Sanofi, Sunpharma, and Novartis, outside the submitted work. E.I.B. serves as a consultant/advisory board member for Pfizer, Werewolf Pharma, Merck, Iovance, Sanofi, Xilio, and Novartis and clinical trial support from Lilly, Novartis, Partners Therapeutics, Genentech, and BVD, outside the submitted work. D.L. has received speaking honorariums and travel fees from Genentech and consulting fees from Oncovalent Therapeutics, not pertinent to or affected by the content of this publication. E.L. served as consultant and/or has received honoraria from Bristol Myers Squibb, Merck Sharp & Dohme, Novartis, Pierre-Fabre, Sanofi, Sunpharma, and Takeda and travel support from Bristol Myers Squibb, Pierre-Fabre, Sunpharma, and Novartis, outside the submitted work. All remaining authors have declared no conflicts of interest. **Patents:** S.F. is a coinventor on patent application US17/634,740 titled "Methods for predicting outcomes of checkpoint inhibition and treatment thereof" related to prediction of melanoma immunotherapy outcomes. F.S.H. has a patent Methods for Treating MICA-Related Disorders (#20100111973) with royalties paid, a patent Tumor antigens and uses thereof (#7250291) issued, a patent Angiopoiten-2 Biomarkers Predictive of Anti-immune checkpoint response (#20170248603) pending, a patent Compositions and Methods for Identification, Assessment, Prevention, and Treatment of Melanoma using PD-L1 Isoforms (#20160340407) pending, a patent Therapeutic peptides (#20160046716) pending, a patent Therapeutic Peptides (#20140004112) pending, a patent Therapeutic Peptides (#20170022275) pending, a patent Therapeutic Peptides (#20170008962) pending, a patent THERAPEUTIC PEPTIDES Therapeutic Peptides Patent number: 9402905 issued, a patent METHODS OF USING PEMBROLIZUMAB AND TREBANANIB pending, a patent Vaccine compositions and methods for restoring NKG2D pathway function against cancers Patent number: 10279021 issued, a patent Antibodies that bind to MHC class I polypeptide-related sequence, a Patent number: 10106611 issued, and a patent ANTI-GALECTIN ANTIBODY BIOMARKERS PREDICTIVE OF ANTI-IMMUNE CHECKPOINT AND ANTI-ANGIOGENESIS RESPONSES. **Data and materials availability:** All analyzed data are in the Supplementary Tables, or data are available on GitHub at https://github.com/davidliu-lab and in Dryad https://doi.org/10.5061/dryad.nzs7h450g. Data to reproduce the work of (*14*), BMS CheckMate-038 and CheckMate-064 findings, and (*33*) cohort have been already published and are included in the Supplementary Table with the same labels. Raw sequencing data of the additional samples included in this analysis are available in dbGaP (accession number phs000452.v4). Code to regenerate figures from the data provided with this study is available at GitHub at https://github.com/davidliu-lab.

Submitted 26 March 2024
Accepted 23 October 2024
Published 27 November 2024
10.1126/sciadv.adp4670